Recent discoveries which strengthen the SKA science case

by Sergei Gulyaev

MYM C4SKA, AUT, 12 July 2018

In the last 2-3 years, a few discoveries were made which some expected to be made by the SKA:

- Protoplanetary discs (ALMA, SPHERE, 2014-2015)
- GW (LIGO, announced on the 1st day of our C4SKA meeting in February 2016)
- The origin of cosmic rays and ultra-energetic neutrinos (mid 2016)
- EoR (2018, right after our S4SKA meeting in February)

Question: Do these discoveries ruin the SKA science case?

- Discoveries do not stop our quest for understanding the material world. Discovery does not “close” the field/area of research. In science each answered question creates new questions.
- New discoveries strengthen the SKA science case. Ideas generated by scientists (in some cases by SKA scientists) are confirmed. We are not working blindly any more. We know where to look on the sky, which frequency, what time domain, and how to design our s/w, receivers and antennas in the most efficient way to answer new questions generated by these discoveries.

Nobel Prizes

- Gravitational waves (GW) – the Nobel Prize of 2017
- EoR – no doubt it will be the NP if/when confirmed.

No Nobel Prizes (NP) to expect from the SKA?

- I wouldn’t worry about it.
- Take discovery of CMB (Arno Pensias and Bob Wilson, 1964; the NP of 1978). The second NP for the CMB went to the COBE team in 2006.
- Pulsars. The NP for the discovery of pulsars, then the NP for discovery of a binary pulsar. Then discovery of a whole class of millisecond pulsars, discovery of a double pulsar. Will there be the NP for discovery and understanding of FRBs?
- By the way, there were two NPs for discovery of GW. The existence of GW was indirectly but firmly proved by the binary pulsar.

- SKA-1 will be more sensitive than SKA precursors (ASKAP, MeerCat, LOFAR, MWA) and provide much greater survey speed. It will be superior to the best Northern Hemisphere radio telescopes and arrays.
- SKA-2 will be 10 times more sensitive and have 50-100 times greater survey speed that modern RTs and arrays.

When a new observational technique appears, which is 1-2 orders of magnitude better that existing, we can expect serendipitous discoveries. Example: Galileo’s telescope vs naked eye.

Not just something “we know that we don’t know”, but also something that we even “don’t know that we don’t know”.

Imaging protoplanetary disks

- One of 5 topics of the KSP#1 “Cradle of Life”

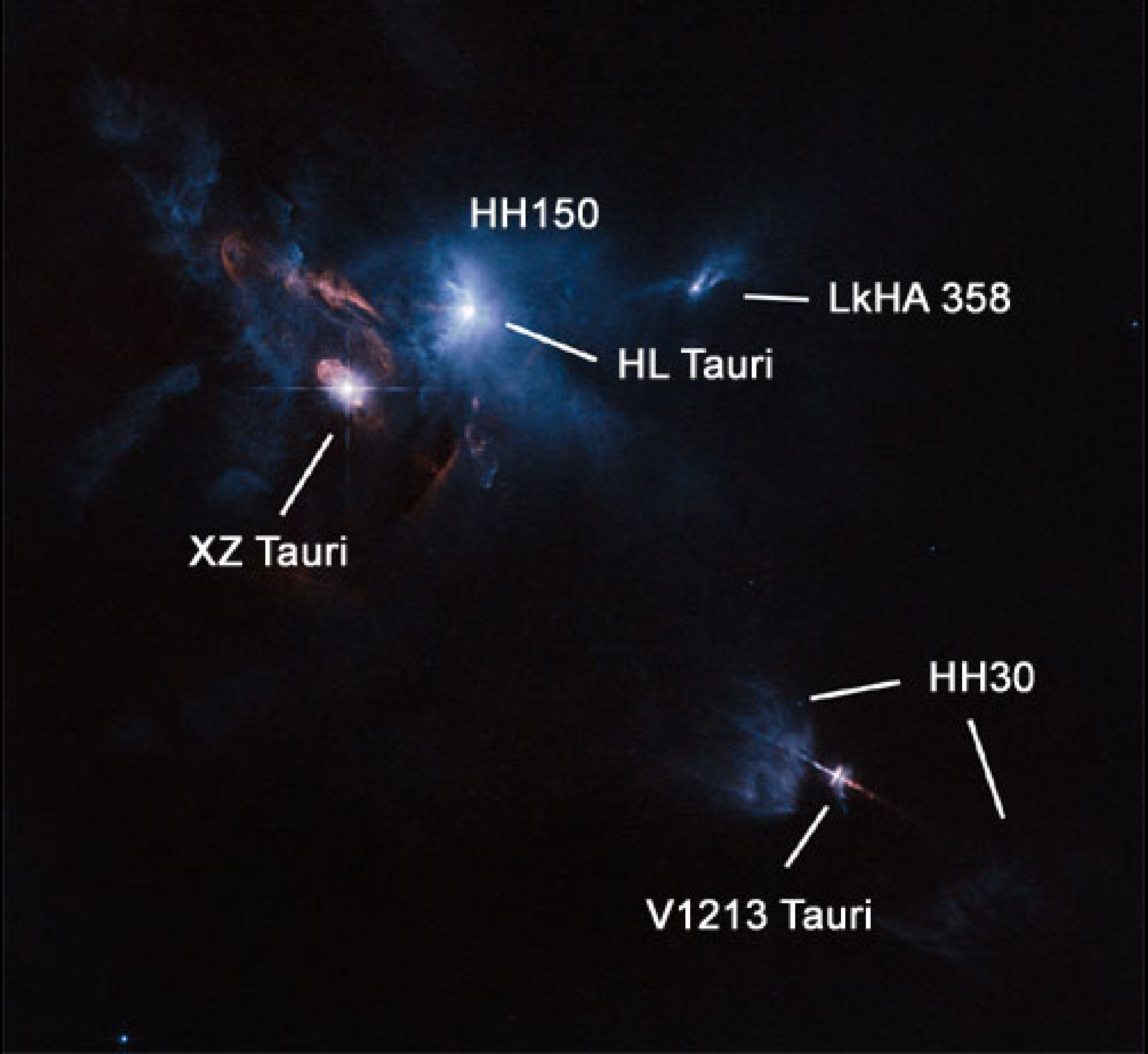
HH150
LkHA 358
HL Tauri
XZ Tauri
HH30
V1213 Tauri

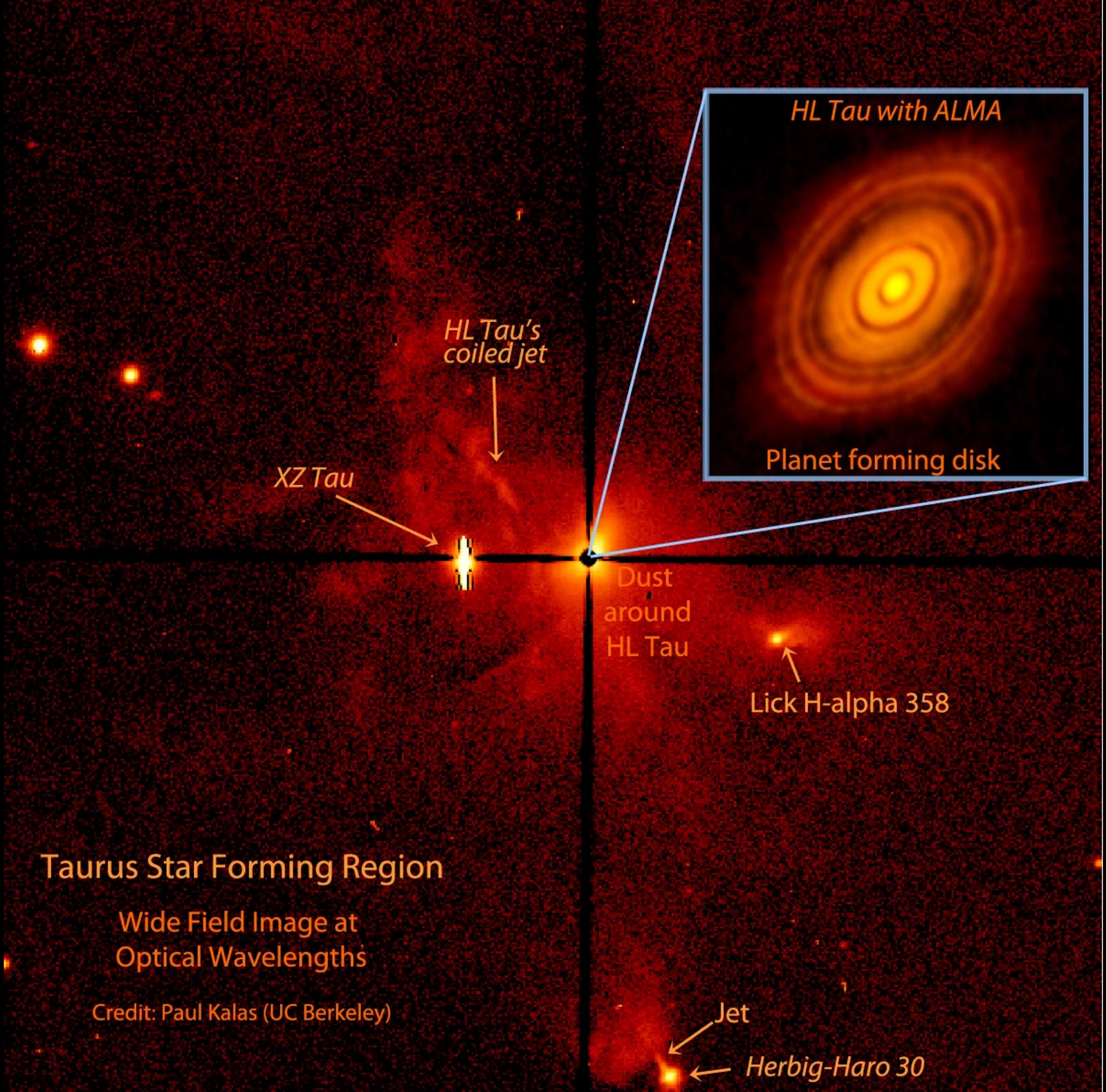
HL Tau with ALMA
Planet forming disk
HL Tau's
coiled jet
XZ Tau
Dust
around
HL Tau
Lick H-alpha 358
Taurus Star Forming Region
Wide Field Image at
Optical Wavelengths
Credit: Paul Kalas (UC Berkeley)
Jet
Herbig-Haro 30

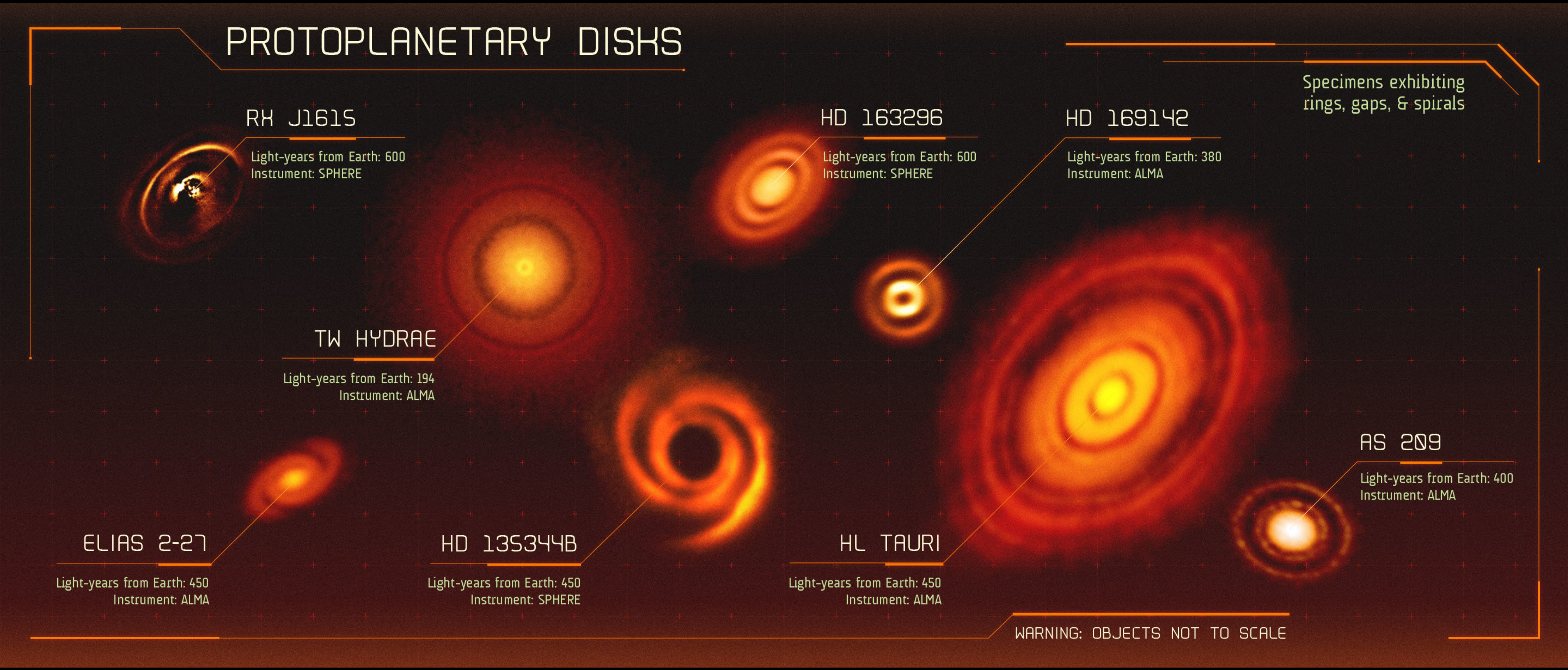
PROTOPLANETARY DISKS
Specimens exhibiting rings, gaps, & spirals
RX J1615
Light-years from Earth: 600
Instrument: SPHERE
HD 163296
Light-years from Earth: 600
Instrument: SPHERE
HD 169142
Light-years from Earth: 380
Instrument: ALMA
TW HYDRAE
Light-years from Earth: 194
Instrument: ALMA
AS 209
Light-years from Earth: 400
Instrument: ALMA
ELIAS 2-27
Light-years from Earth: 450
Instrument: ALMA
HD 135344B
Light-years from Earth: 450
Instrument: SPHERE
HL TAURI
Light-years from Earth: 450
Instrument: ALMA
WARNING: OBJECTS NOT TO SCALE

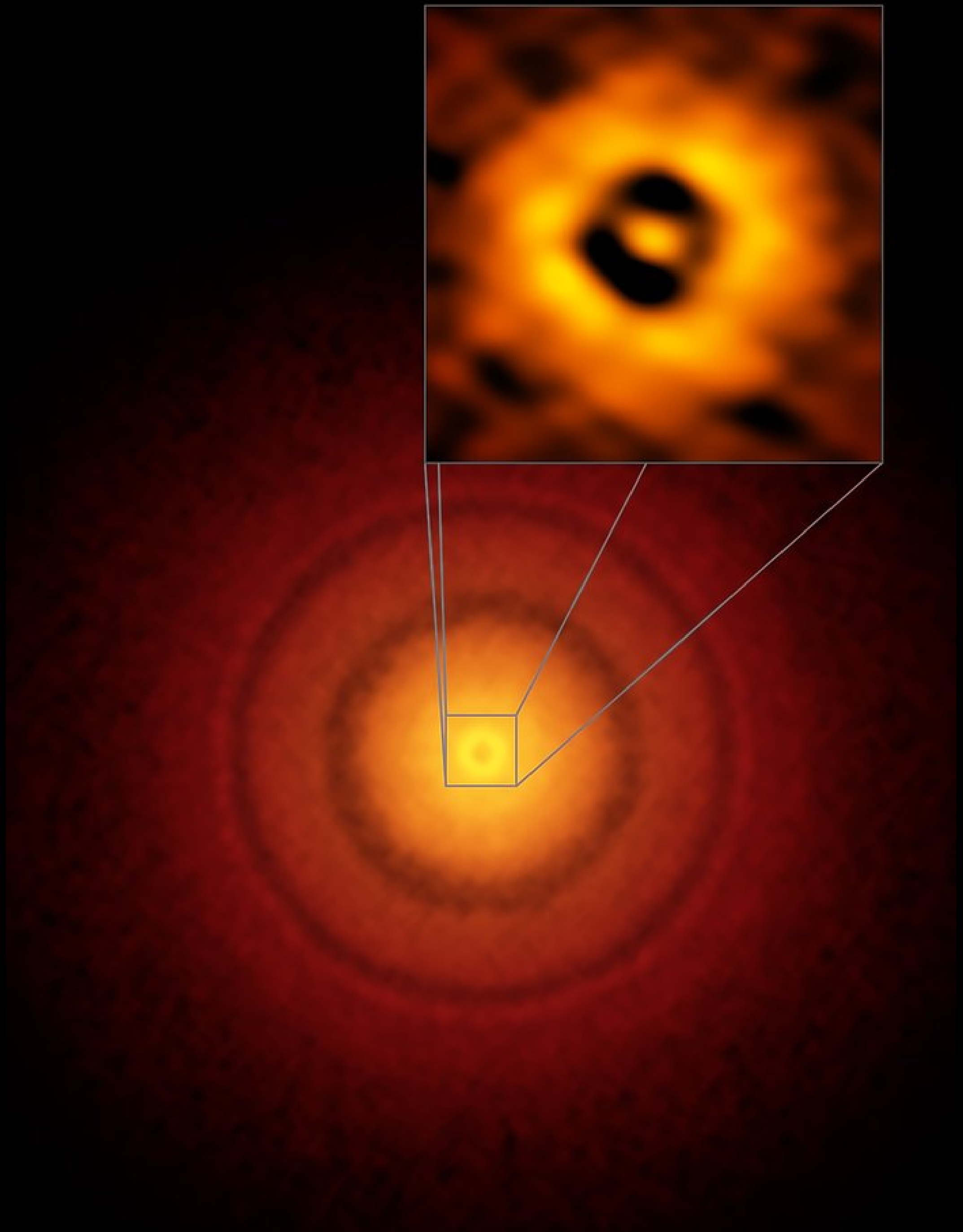

ALMA image of the planet-forming disc around the young, Sun-like star TW Hydrae. The inset image (upper right) zooms in on the gap nearest to the star, which is at the same distance as the Earth is from the Sun, suggesting an infant version of our home planet could be emerging from the dust and gas. The additional concentric light and dark features represent other planet-forming regions farther out in the disc.

Credit: S. Andrews (Harvard-Smithsonian CfA), ALMA (ESO/NAOJ/NRAO)

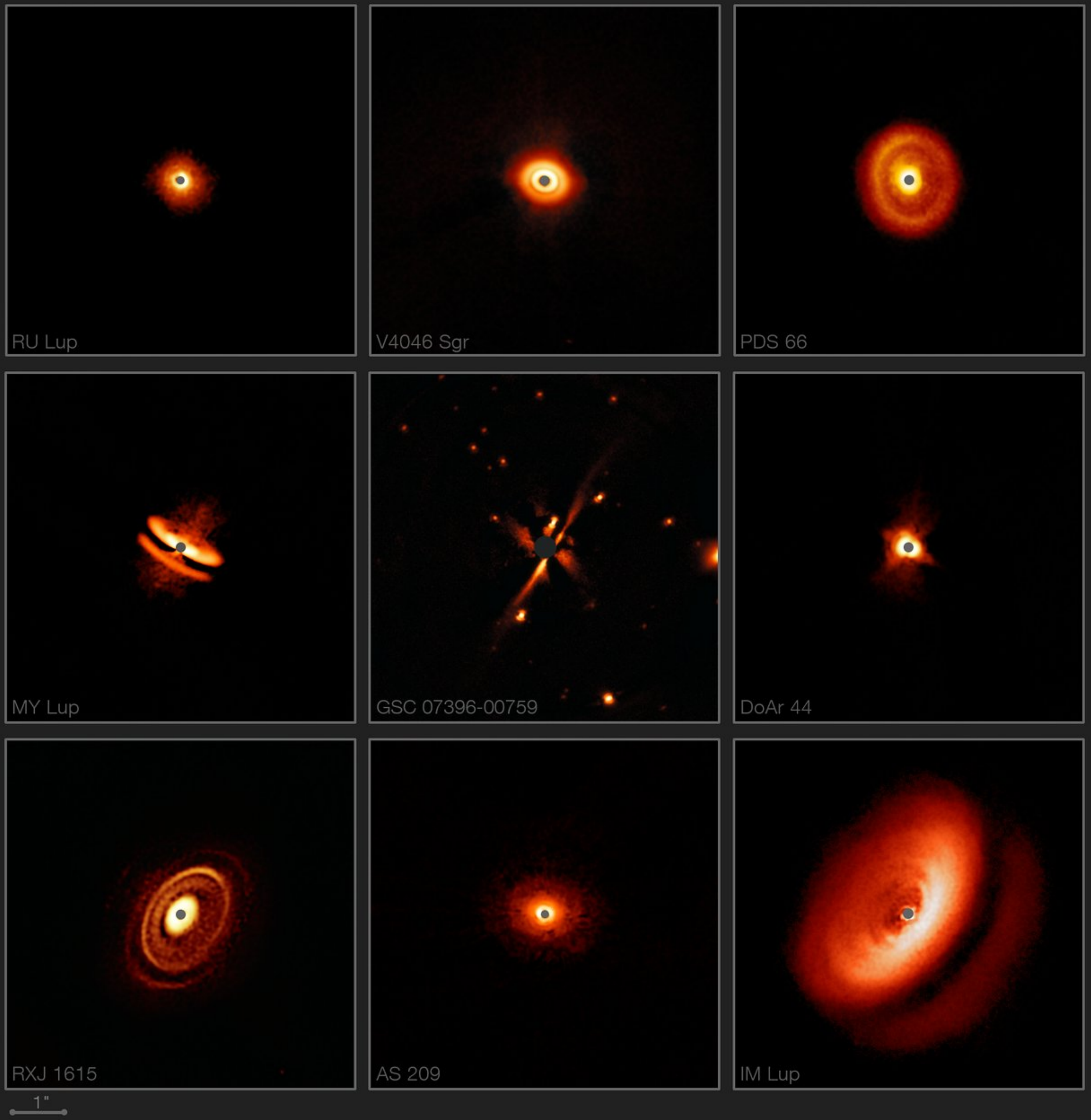

SPHERE (VLT in Chile)

- The Cradle of Life topics with the SKA-1:
    - Dust evolution and grain growth in proto-planetary discs (up to cm-size particles, compared to just submm-size with ALMA);
    - Snow line detection in proto-planetary discs;
    - Complex organic and pre-biotic (amino acid) molecules in proto-planetary discs (e.g. alpha-alanine, glycine, etc.);
    - Measuring magnetic fields of exoplanets and habitability;
    - Temperament of young stars (flares, stellar wind) and its effect on p-p discs;
    - SETI (radars, broadcasts, etc.)

Gravitational waves

- The existence of GW was proved indirectly, but firmly by measurements of properties of the binary pulsar PKS1913+16 discovered in 1974 by Jo Taylor and his PhD student Russell Hulse (the NP of 1993).
- Similar to our discussion on the SKA, the question arose – should money be spent on construction of LIGO detector, and then its space version LISA.

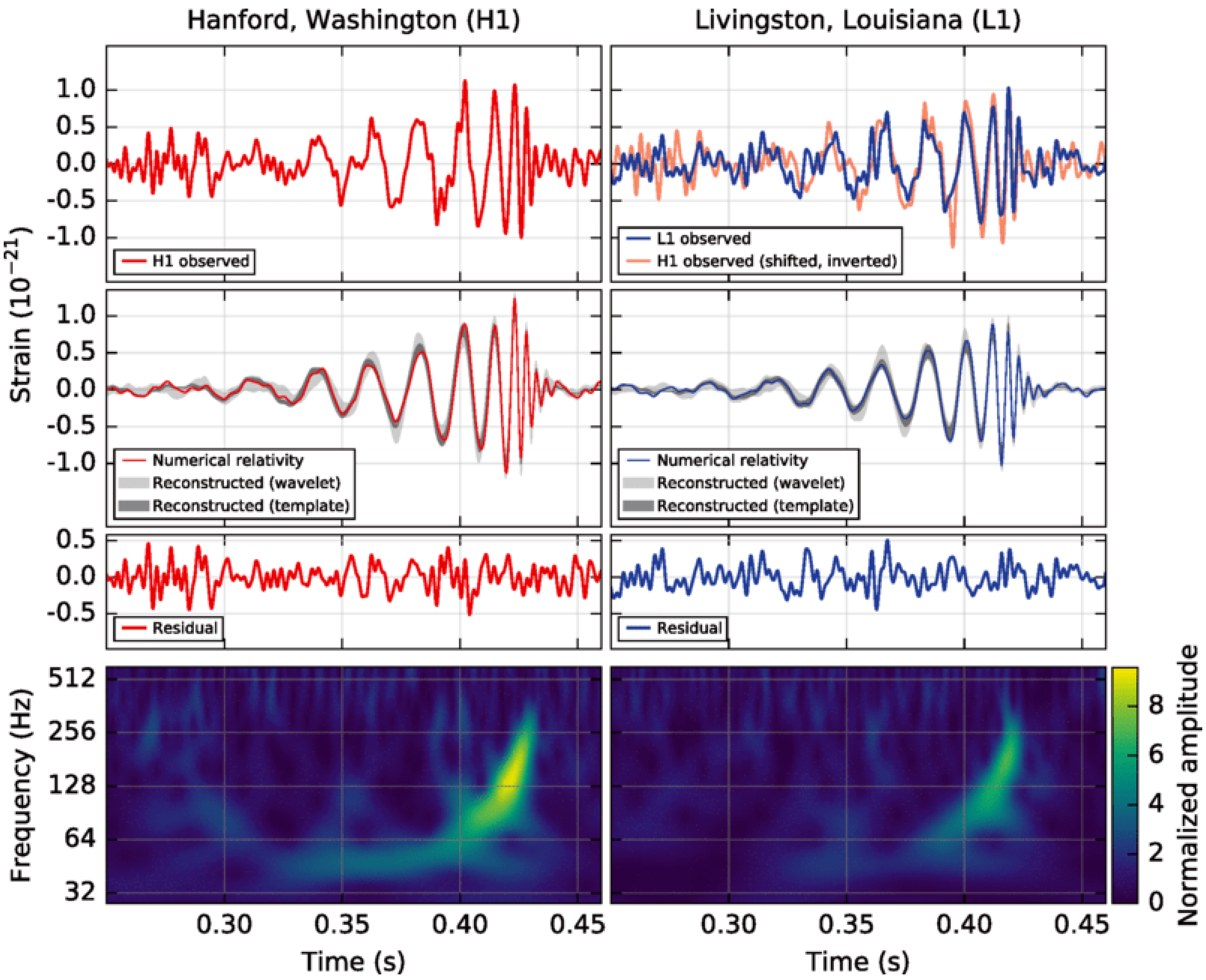

GW150914 – 14 Sep 2015

- No identification for the GW150914
- The first identification two years later – GW170817 (EM170817)

Illuminating Gravitational Waves: A Concordant Picture of Photons from a Neutron Star Merger

M. M. Kasliwal[1*], E. Nakar[2], L. P. Singer[3,4], D. L. Kaplan[5], D. O. Cook[1], A. Van Sistine[5], R. M. Lau[1], C. Fremling[1], O. Gottlieb[2], J. E. Jencson[1], S.M. Adams[1], U. Feindt[6], K. Hotokezaka[7], S. Ghosh[5], D. A. Perley[8], P.-C. Yu[9], T. Piran[10], J. R. Allison[11,12], G. C. Anupama[13], A.Balasubramanian[14], K. W Bannister[15], J. Bally[16], J. Barnes[17], S. Barway[18], E.

October 2017

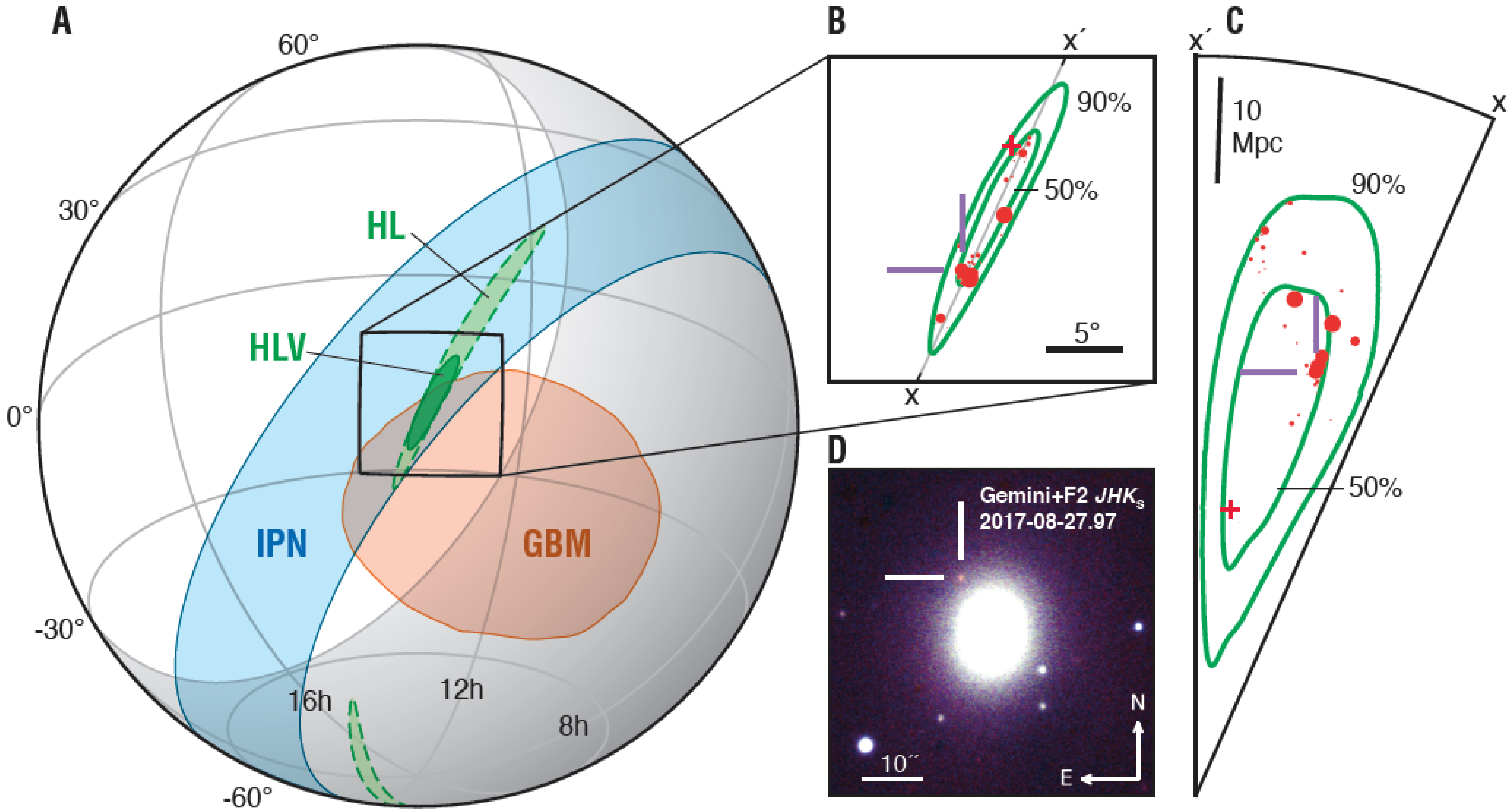

A
60°
30°
0°
-30°
-60°
HL
HLV
IPN
GBM
16h
12h
8h
B
x´
x
90%
50%
5°
C
x´
x
10
Mpc
90%
50%
D
Gemini+F2 JHKs
2017-08-27.97
10´´
N
E

Gemini:

Two 8.1-m optical/IR telescopes in Hawaii and Chile

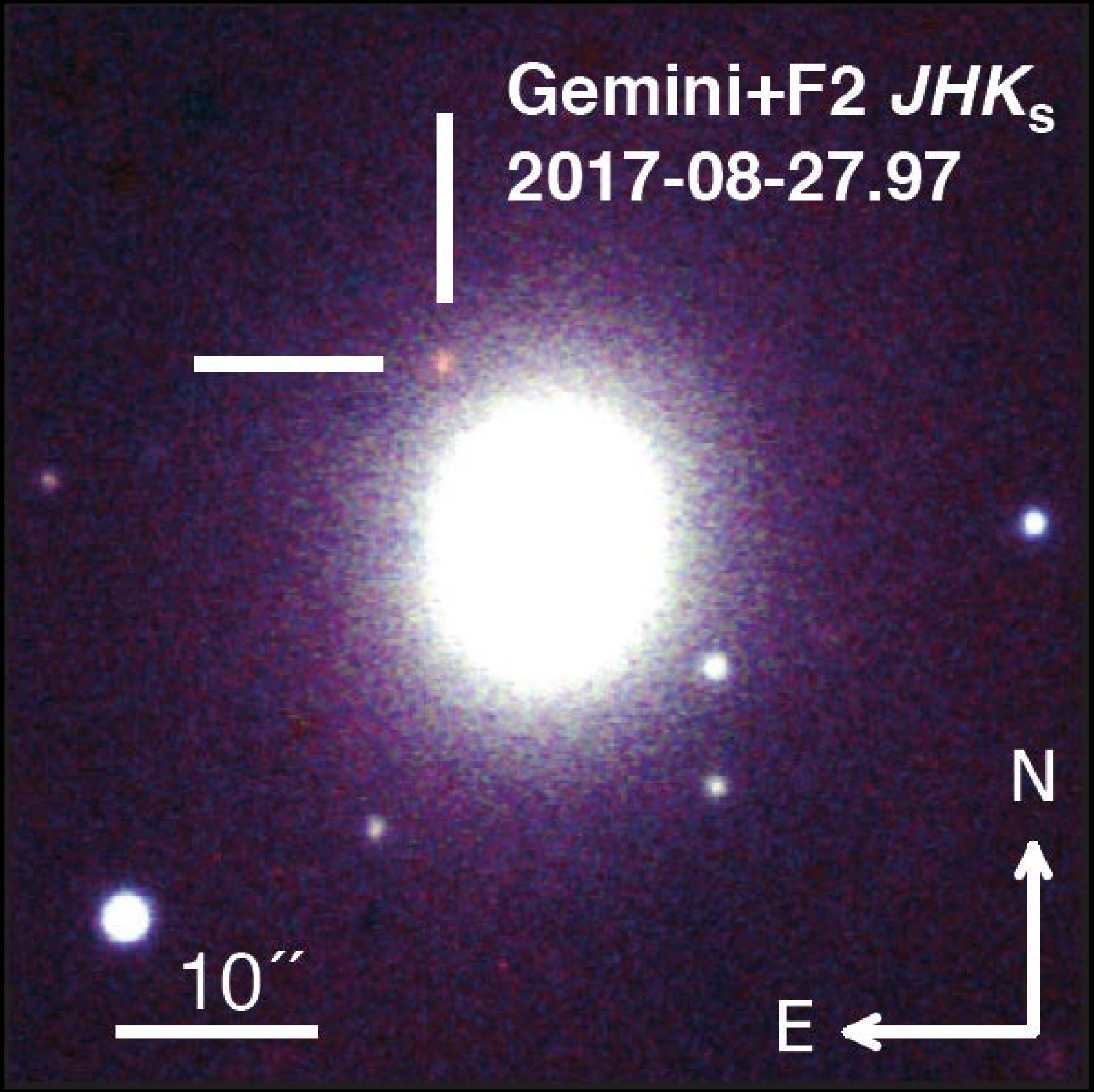

NGC4993

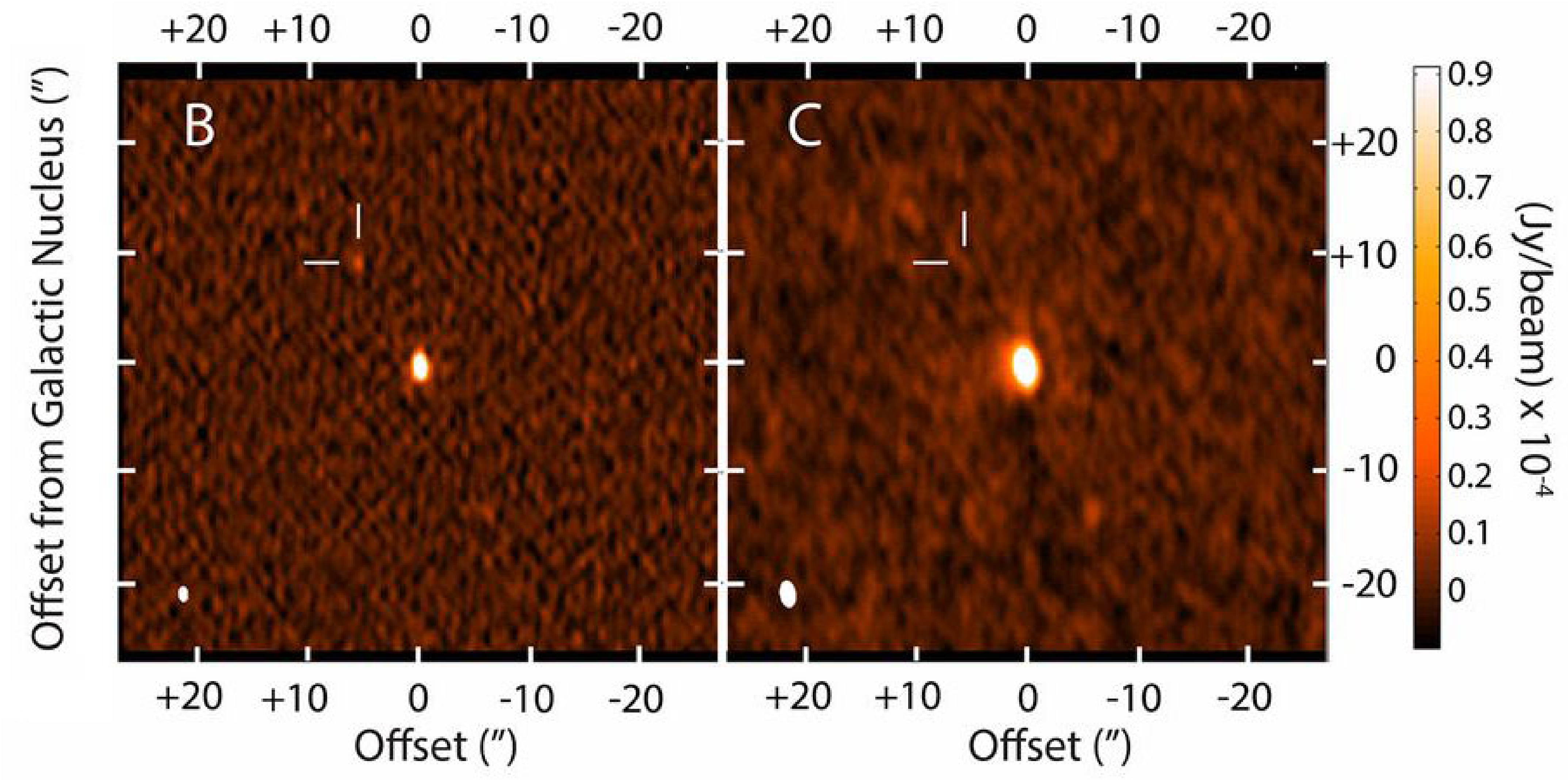

[Left] Radio image created using VLA observations (6 GHz) on 9 September 2017, with the radio counterpart to EM170817 highlighted. Its flux density is 23 ± 3.4 μJy. **[Right]** A combined image from four VLA observations at 6 GHz spanning 22.6 August–1 September 2017. The flux density at the position of EM170817 is 7.8 ± 2.6 μJy, consistent with a marginal or non-detection.

- A burst of gamma-rays, GRB170817A, was detected ~2 seconds after the GW detection the Fermi Gamma-ray Space Telescope. The GW source was localized to an area of 28 deg^2 and a distance of 40 ± 8 Mpc.
- There were 49 cataloged galaxies within this volume, allowing astronomers to rapidly search for electromagnetic counterparts. An optical counterpart, designated SSS17a, was detected within ~11 hours of the GW event, in the S0-type galaxy NGC 4993 at a distance of 40 Mpc and soon independently confirmed.
- The radio afterglow was registered using the Jansky VLA and ATCA 16 days after the GW burst!

UT Date	ΔT (d)	Telescope	ν (GHz)	Bandwidth (GHz)	S_ν (mJy)
Aug 18.21	0.68	ATCA	8.5	2.049	< 0.120
Aug 18.21	0.68	ATCA	10.5	2.049	< 0.150
Aug 18.46	0.93	GMRT	0.61	0.032	< 0.195
Aug 18.92	1.39	VLA	10	3.8	<0.0154†
Aug 18.97	1.44	VLITE/VLA	0.3387	0.034	< 34.8
Aug 19.95	2.42	VLA	6.2	4	< 0.020
Aug 19.95	2.42	VLA	9.7	4	< 0.017
Aug 19.95	2.42	VLA	15	6	< 0.022
Aug 19.97	2.44	VLITE/VLA	0.3387	0.034	< 28.8
Aug 20.31	2.78	GMRT	0.4	0.2	< 0.780
Aug 20.46	2.93	GMRT	1.2	0.4	< 0.098

UT Date	ΔT (d)	Telescope	ν (GHz)	Bandwidth (GHz)	S_ν (mJy)
Aug 20.87	3.34	VLA	3	1.6	< 0.032
Aug 20.87	3.34	VLITE/VLA	0.3387	0.034	< 44.7
Aug 21.23	3.7	ATCA	8.5	2.049	< 0.135
Aug 21.23	3.7	ATCA	10.5	2.049	< 0.099
Aug 22.88	5.35	VLA	6.2	4	< 0.019
Aug 25.90	8.37	VLITE/VLA	0.3387	0.034	< 37.5
Aug 27.90	10.37	VLA	6.2	4	0.0078 ± 0.0026*
Aug 28.18	10.65	ATCA	8.5	2.049	< 0.054
Aug 28.18	10.65	ATCA	10.5	2.049	< 0.039
Aug 29.45	11.92	GMRT	0.7	0.4	< 0.123
Aug 30.98	13.45	VLA	6.2	4	< 0.023

UT Date	ΔT (d)	Telescope	ν (GHz)	Bandwidth (GHz)	S_ν (mJy)
Aug 30.98	13.45	VLITE/VLA	0.3387	0.034	< 20.4
Aug 31.46	13.93	GMRT	0.4	0.2	< 0.600
Sep 01.89	15.37	VLA	6.2	4	< 0.013
Sep 01.90	15.37	VLITE/VLA	0.3387	0.034	< 11.4
Sep 02.89	16.36	VLITE/VLA	0.3387	0.034	< 11.7
Sep 02.95	16.42	VLA	3	2	0.0187 ± 0.0063
Sep 03.01	16.48	VLA	6.2	4	0.0283 ± 0.0054
Sep 03.92	17.39	VLA	3	2	0.0151 ± 0.0039
Sep 03.93	17.4	VLITE/VLA	0.3387	0.034	< 6.9
Sep 04.86	18.33	VLA	3	2	0.0145 ± 0.0037
Sep 05.18	18.66	ATCA	7.25	4.098‡	0.025 ± 0.006

UT Date	ΔT (d)	Telescope	ν (GHz)	Bandwidth (GHz)	S_ν (mJy)
Sep 05.52	18.99	GMRT	0.7	0.4	< 0.140
Sep 05.88	19.35	VLA	6.2	4	0.0159 ± 0.0055
Sep 07.89	21.36	VLA	6.2	4	0.0136 ± 0.0029
Sep 07.89	21.36	VLITE/VLA	0.3387	0.034	< 8.1
Sep 08.89	22.36	VLA	3	2	0.0225 ± 0.0034
Sep 08.90	22.37	VLITE/VLA	0.3387	0.034	< 6.3
Sep 09.89	23.36	VLITE/VLA	0.3387	0.034	< 4.8
Sep 09.89	23.36	VLA	6	4	0.0226 ± 0.0034
Sep 10.79	24.26	VLA	3	2	0.0256 ± 0.0029
Sep 10.88	24.35	VLITE/VLA	0.3387	0.034	< 6.6
Sep 17.75	31.22	VLA	3	2	0.034 ± 0.0036

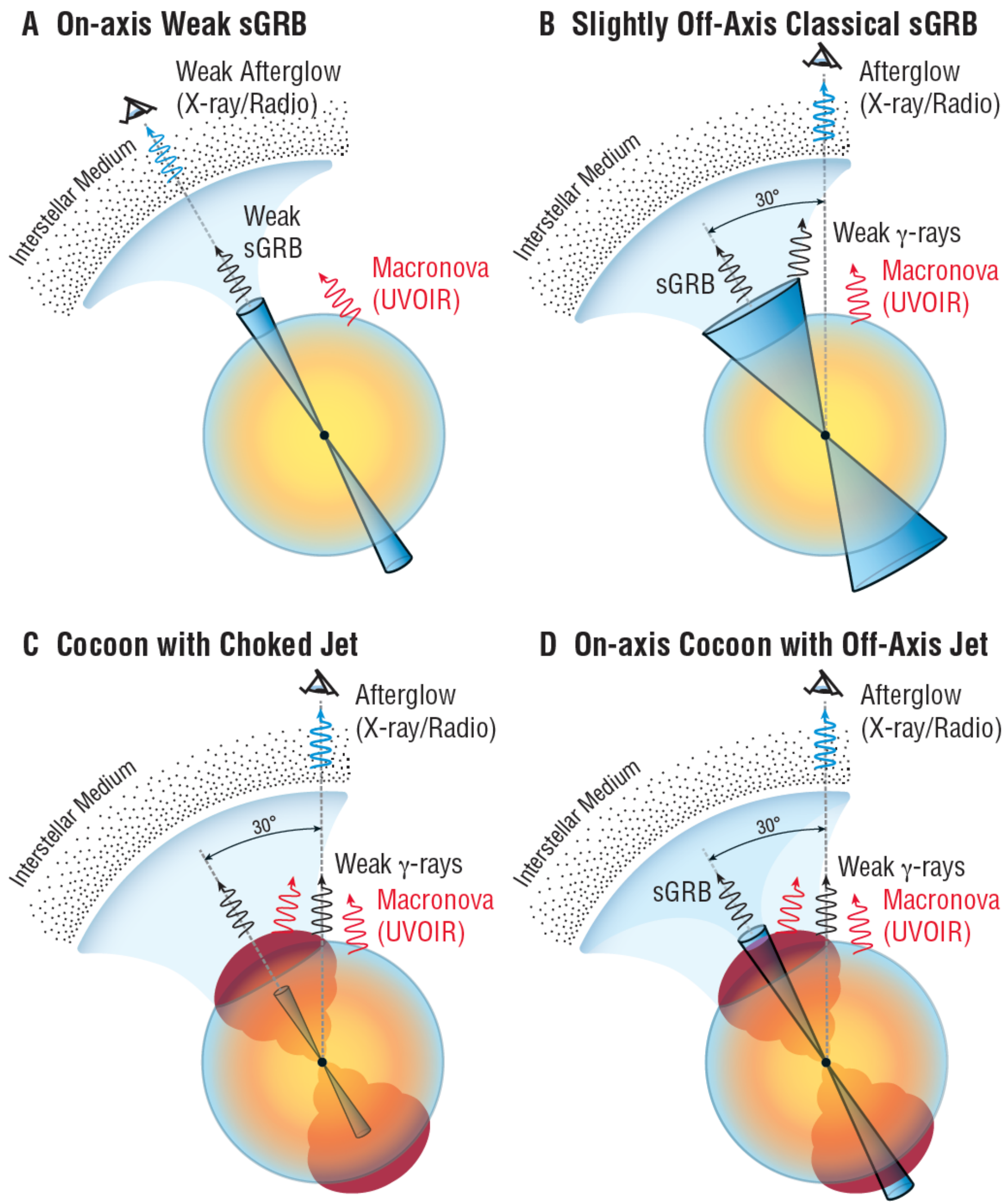
A On-axis Weak sGRB
Weak Afterglow
(X-ray/Radio)
Interstellar Medium
Weak
sGRB
Macronova
(UVOIR)
B Slightly Off-Axis Classical sGRB
Afterglow
(X-ray/Radio)
Interstellar Medium
30°
Weak γ-rays
sGRB
Macronova
(UVOIR)
C Cocoon with Choked Jet
Afterglow
(X-ray/Radio)
Interstellar Medium
30°
Weak γ-rays
Macronova
(UVOIR)
D On-axis Cocoon with Off-Axis Jet
Afterglow
(X-ray/Radio)
Interstellar Medium
30°
Weak γ-rays
sGRB
Macronova
(UVOIR)

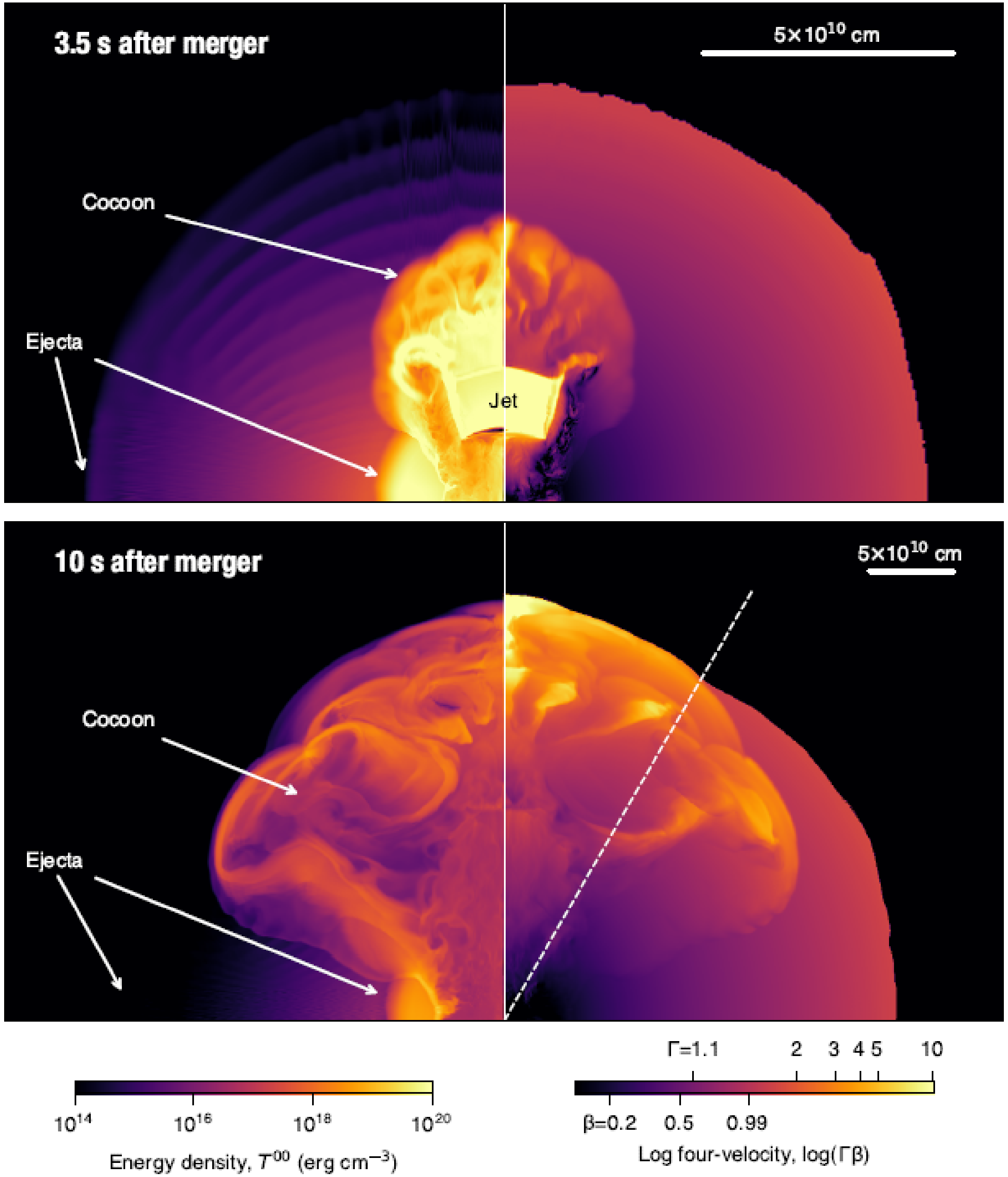
3.5 s after merger
5×10^10 cm
Cocoon
Ejecta
Jet
10 s after merger
5×10^10 cm
Cocoon
Ejecta
10^14
10^16
10^18
10^20
Energy density, T^00 (erg cm^−3)
Γ=1.1
2
3
4
5
10
β=0.2
0.5
0.99
Log four-velocity, log(Γβ)

SKA GW are different

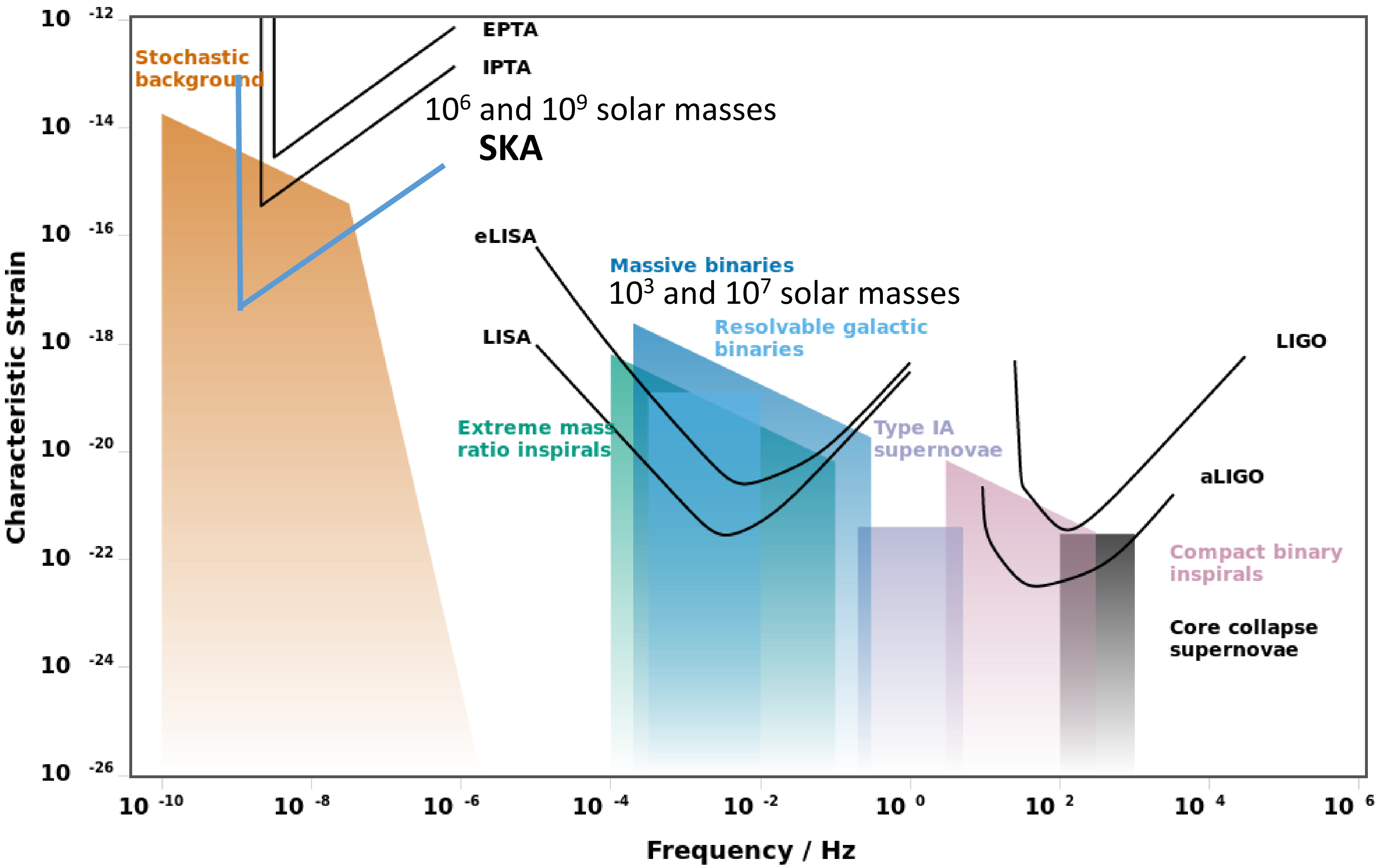

- We expect SKA will discover merger of supermassive BHs
- Determine properties of GW, spectrum of GW
- There will be a very important role of optical and gamma-ray telescopes, as well as of VLBI in identification of the object responsible for the event.

The origin of cosmic rays (incl. ultra-energetic neutrinos)

Cosmic rays: high-energy particles

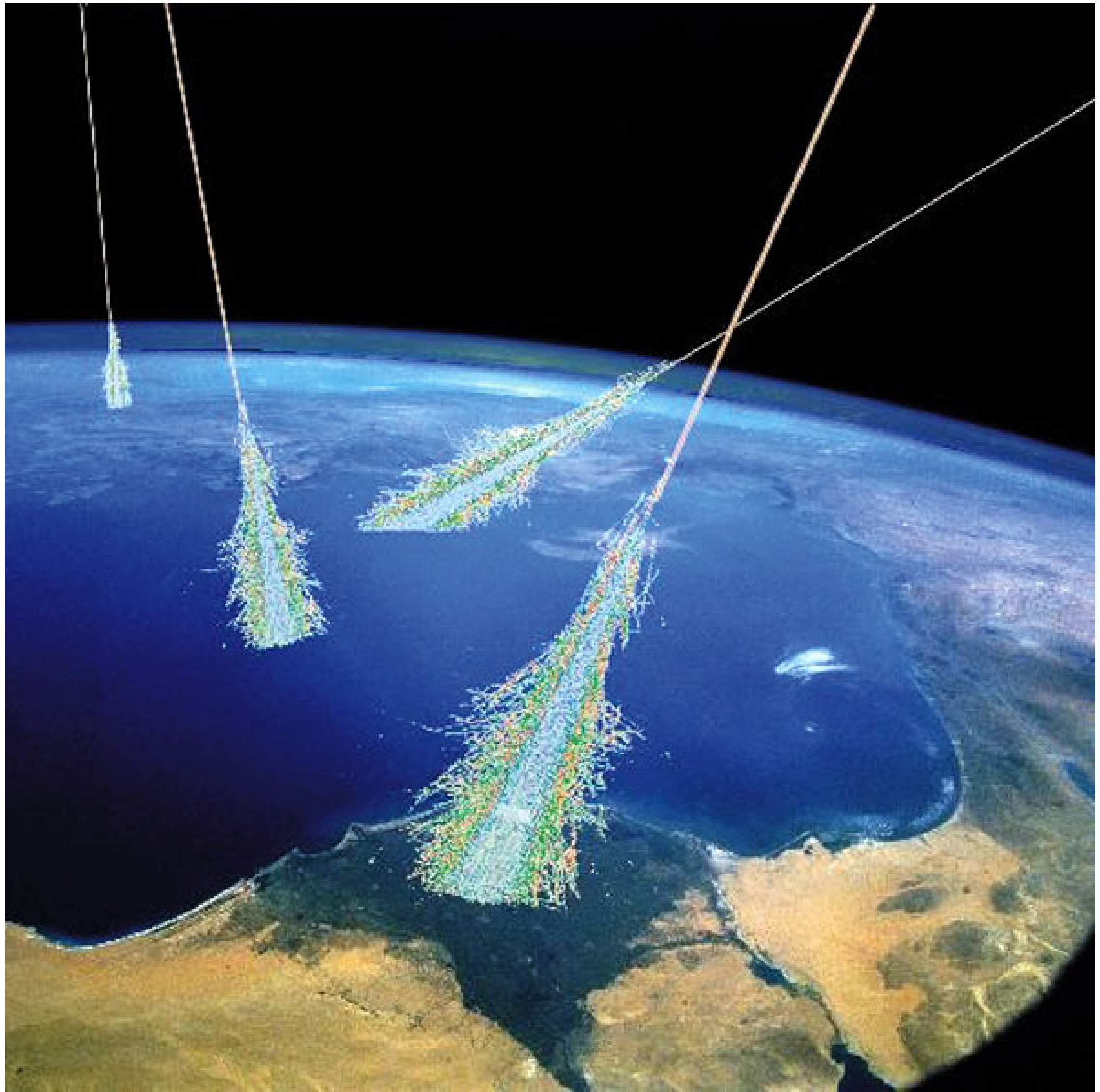

The most energetic ultra-high-energy cosmic rays (UHECRs) have been observed to approach 3×10^{20} eV, about 40 million times the energy of particles accelerated by the Large Hadron Collider and 20 million times the energy of photos ever detected.

Oh-My-God particle (a proton):
99.99999999999999999999951% of the speed of light.

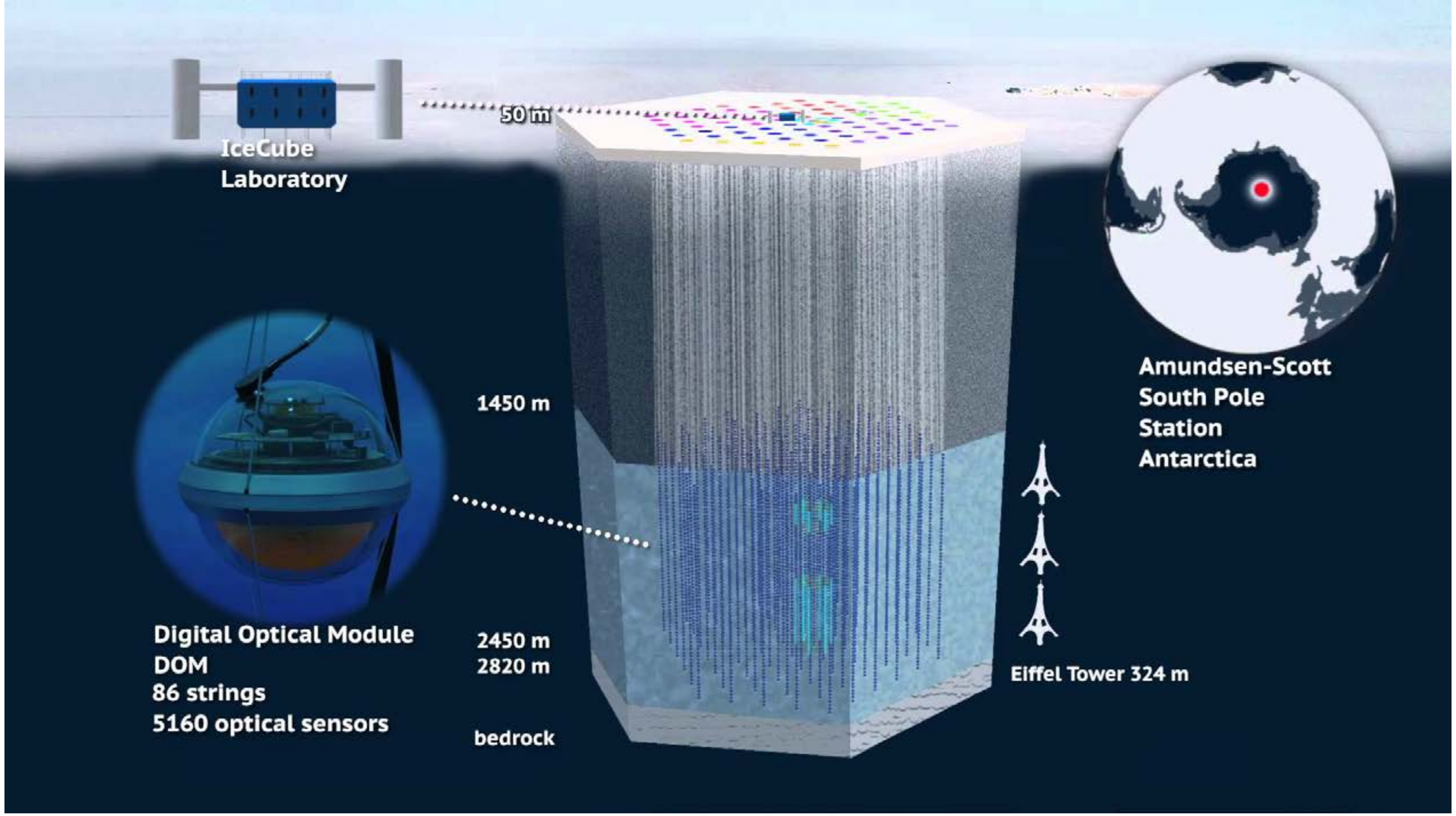

50 m
IceCube Laboratory
Amundsen-Scott South Pole Station Antarctica
1450 m
2450 m
2820 m
bedrock
Eiffel Tower 324 m
Digital Optical Module DOM
86 strings
5160 optical sensors

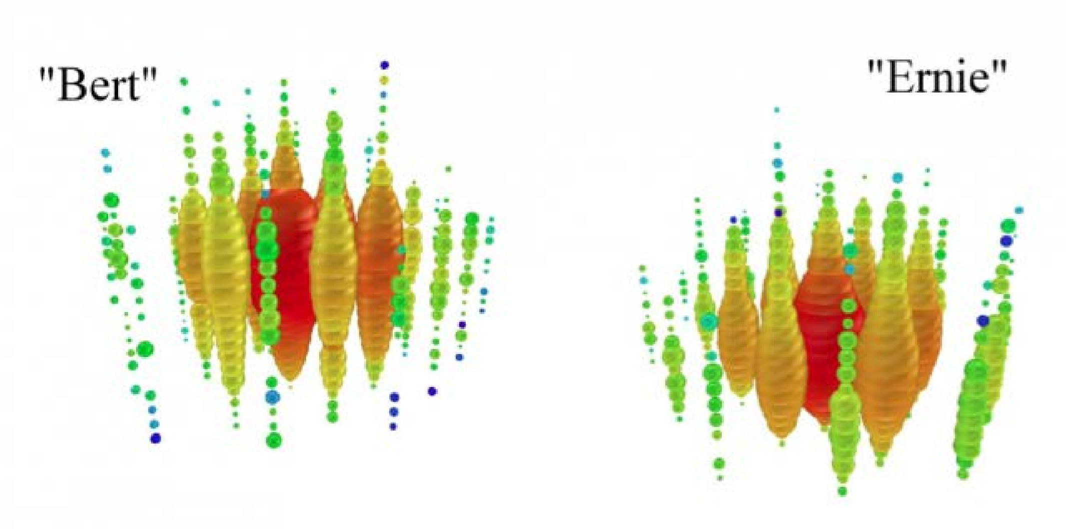
"Bert"
"Ernie"

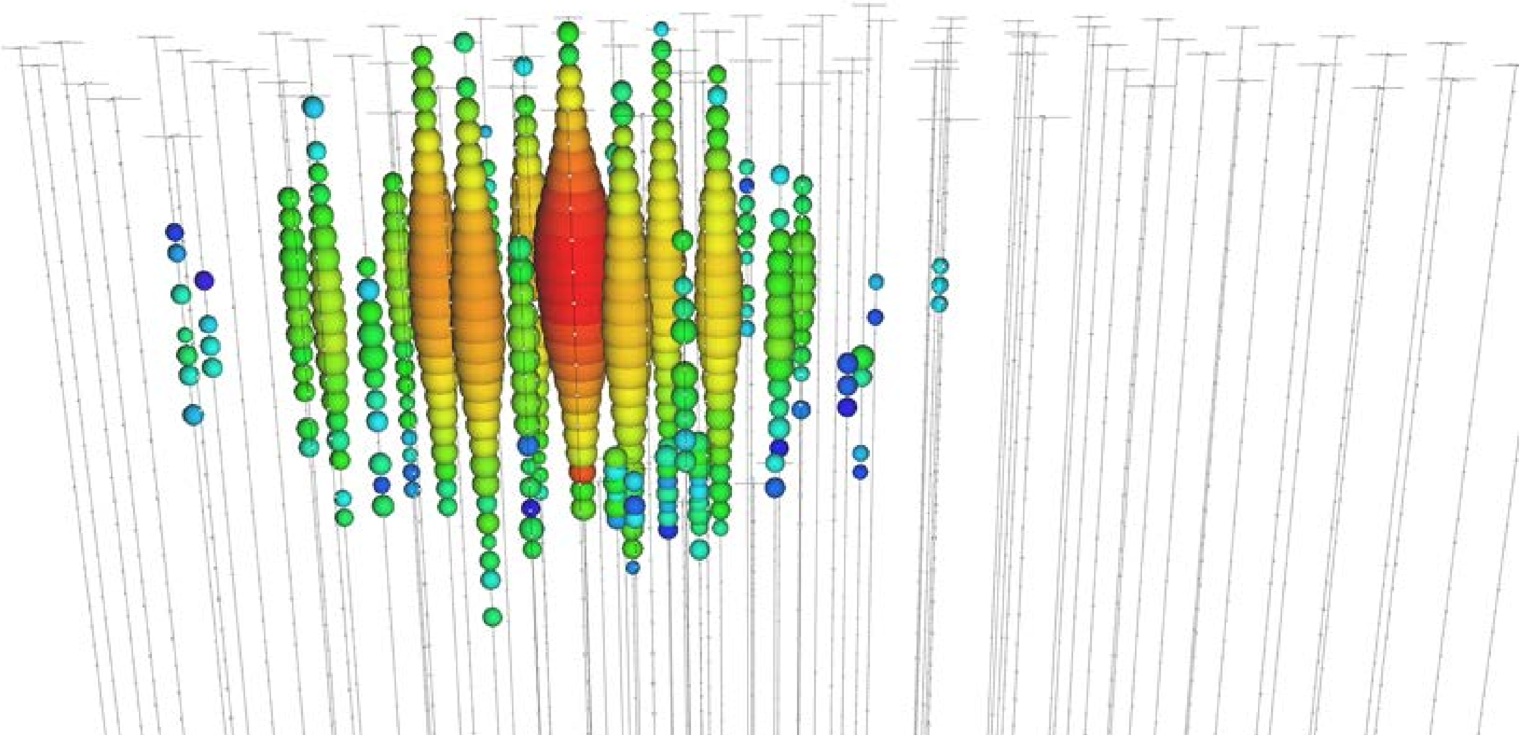

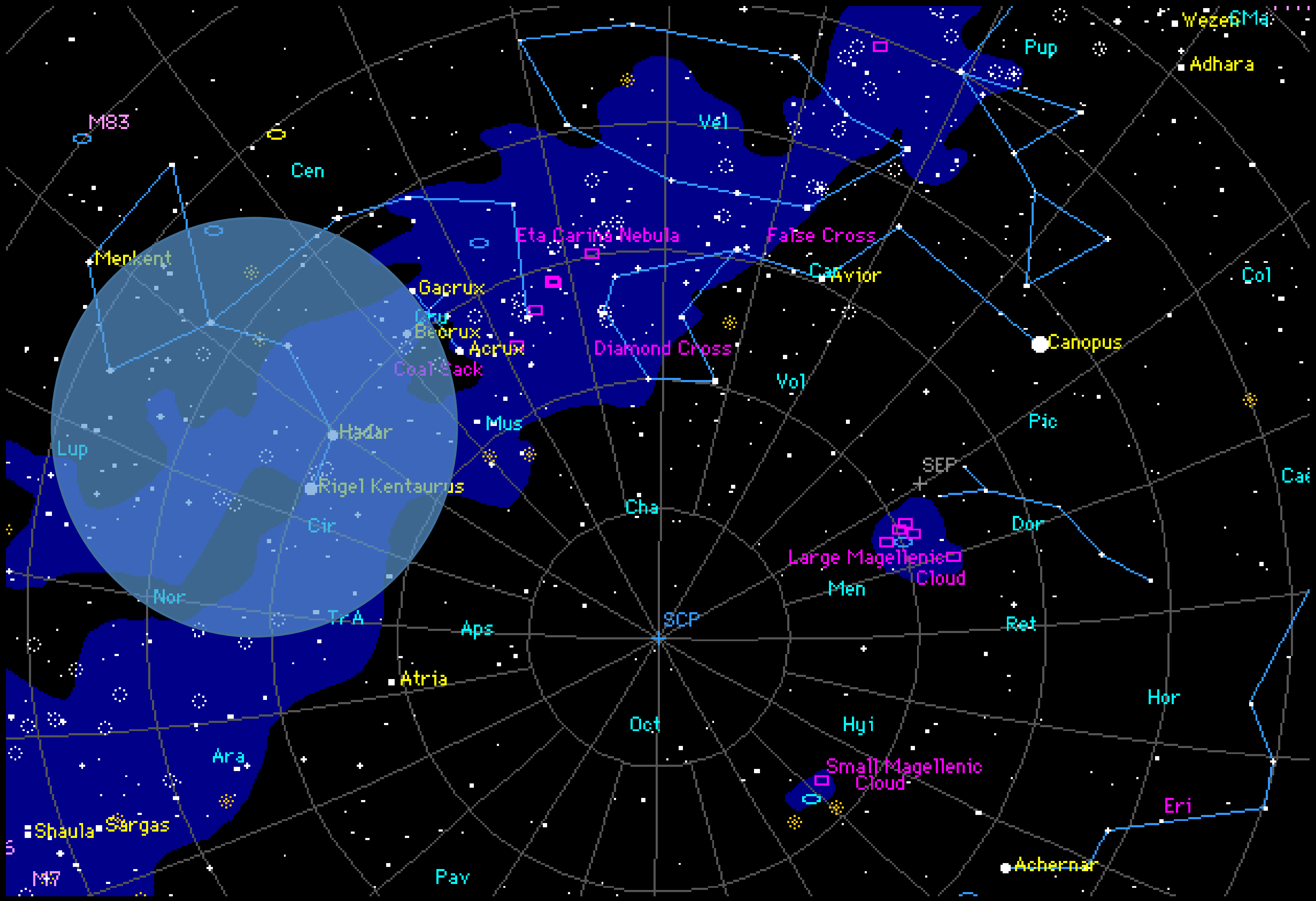
M83
Cen
Menkent
Gacrux
Cru
Becrux
Acrux
Coal Sack
Hadar
Rigel Kentaurus
Lup
Cir
Nor
TrA
Mus
Eta Carina Nebula
Vel
False Cross
Car
Avior
Diamond Cross
Vol
Pup
Wezen
CMa
Adhara
Canopus
Col
Pic
SEP
Dor
Cae
Cha
Large Magellenic Cloud
Men
SCP
Ret
Aps
Atria
Oct
Hyi
Hor
Small Magellenic Cloud
Eri
Achernar
Ara
Shaula
Sargas
M7
Pav

fermi
Gamma-ray
Space Telescope

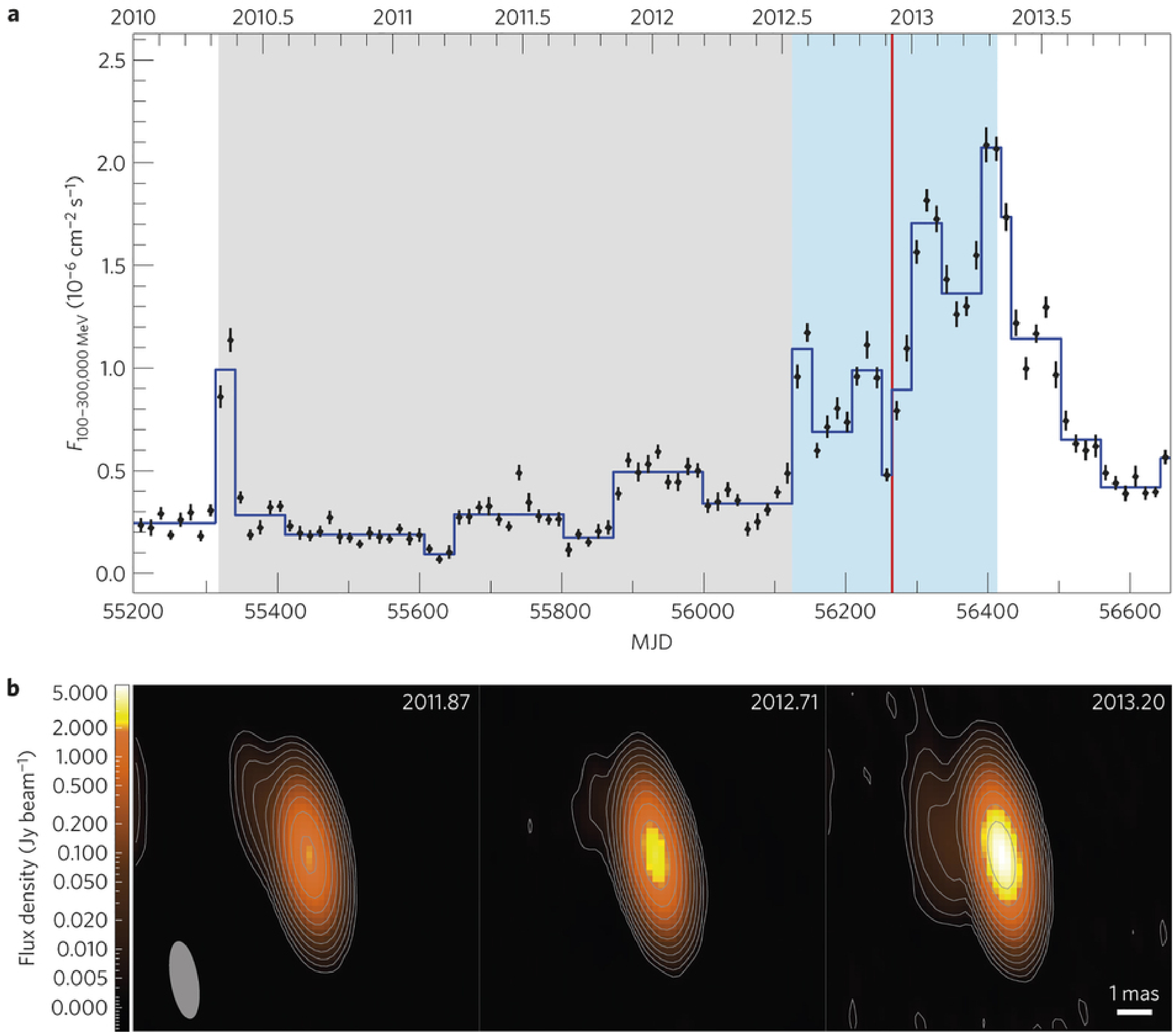
a
2010
2010.5
2011
2011.5
2012
2012.5
2013
2013.5
$F_{100-300,000\ \mathrm{MeV}}$ (10^{-6} cm^{-2} s^{-1})
2.5
2.0
1.5
1.0
0.5
0.0
55200
55400
55600
55800
56000
56200
56400
56600
MJD
b
Flux density (Jy beam^{-1})
5.000
2.000
1.000
0.500
0.200
0.100
0.050
0.020
0.010
0.005
0.000
2011.87
2012.71
2013.20
1 mas

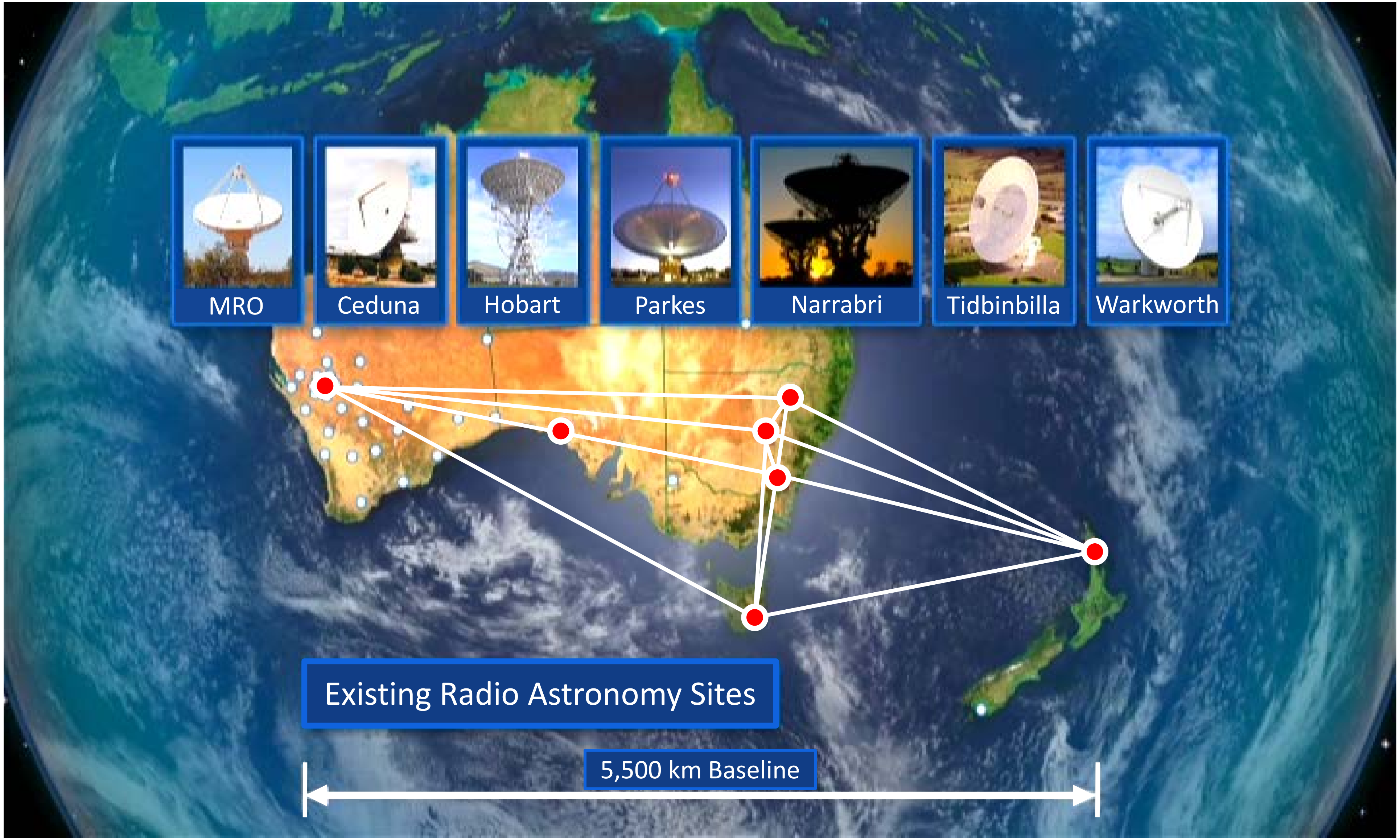
MRO
Ceduna
Hobart
Parkes
Narrabri
Tidbinbilla
Warkworth
Existing Radio Astronomy Sites
5,500 km Baseline

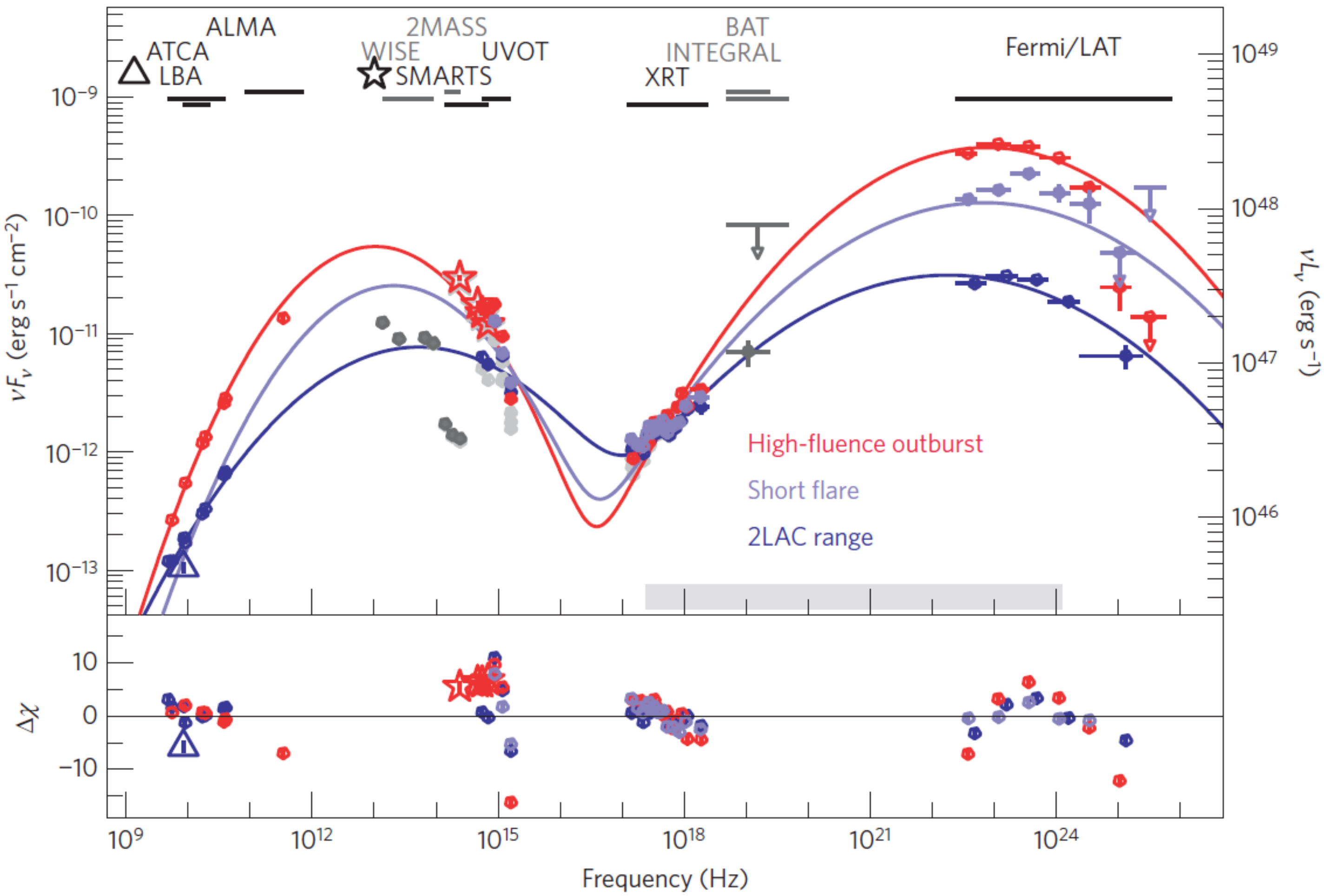

ALMA
ATCA
LBA
2MASS
WISE
UVOT
SMARTS
BAT
INTEGRAL
XRT
Fermi/LAT
High-fluence outburst
Short flare
2LAC range
νF_ν (erg s^{-1} cm^{-2})
νL_ν (erg s^{-1})
$\Delta\chi$
Frequency (Hz)

nature physics

ARTICLES

PUBLISHED ONLINE: 18 APRIL 2016 | DOI: 10.1038/NPHYS3715

Coincidence of a high-fluence blazar outburst with a PeV-energy neutrino event

M. Kadler[1*], F. Krauß[1,2], K. Mannheim[1], R. Ojha[3,4,5], C. Müller[1,6], R. Schulz[1,2], G. Anton[7], W. Baumgartner[3], T. Beuchert[1,2], S. Buson[8,9], B. Carpenter[5], T. Eberl[7], P. G. Edwards[10], D. Eisenacher Glawion[1], D. Elsässer[1], N. Gehrels[3], C. Gräfe[1,2], S. Gulyaev[11], H. Hase[12], S. Horiuchi[13], C. W. James[7], A. Kappes[1], A. Kappes[7], U. Katz[7], A. Kreikenbohm[1,2], M. Kreter[1,7], I. Kreykenbohm[2], M. Langejahn[1,2], K. Leiter[1,2], E. Litzinger[1,2], F. Longo[14,15], J. E. J. Lovell[16], J. McEnery[3], T. Natusch[11], C. Phillips[10], C. Plötz[12], J. Quick[17], E. Ros[18,19,20], F. W. Stecker[3,21], T. Steinbring[1,2], J. Stevens[10], D. J. Thompson[3], J. Trüstedt[1,2], A. K. Tzioumis[10], S. Weston[11], J. Wilms[2] and J. A. Zensus[18]

The astrophysical sources of the extraterrestrial, very high-energy neutrinos detected by the IceCube collaboration remain to be identified. Gamma-ray (γ-ray) blazars have been predicted to yield a cumulative neutrino signal exceeding the atmospheric background above energies of 100 TeV, assuming that both the neutrinos and the γ-ray photons are produced by accelerated protons in relativistic jets. As the background spectrum falls steeply with increasing energy, the individual events with the clearest signature of being of extraterrestrial origin are those at petaelectronvolt energies. Inside the large positional-uncertainty fields of the first two petaelectronvolt neutrinos detected by IceCube, the integrated emission of the blazar population has a sufficiently high electromagnetic flux to explain the detected IceCube events, but fluences of individual objects are too low to make an unambiguous source association. Here, we report that a major outburst of the

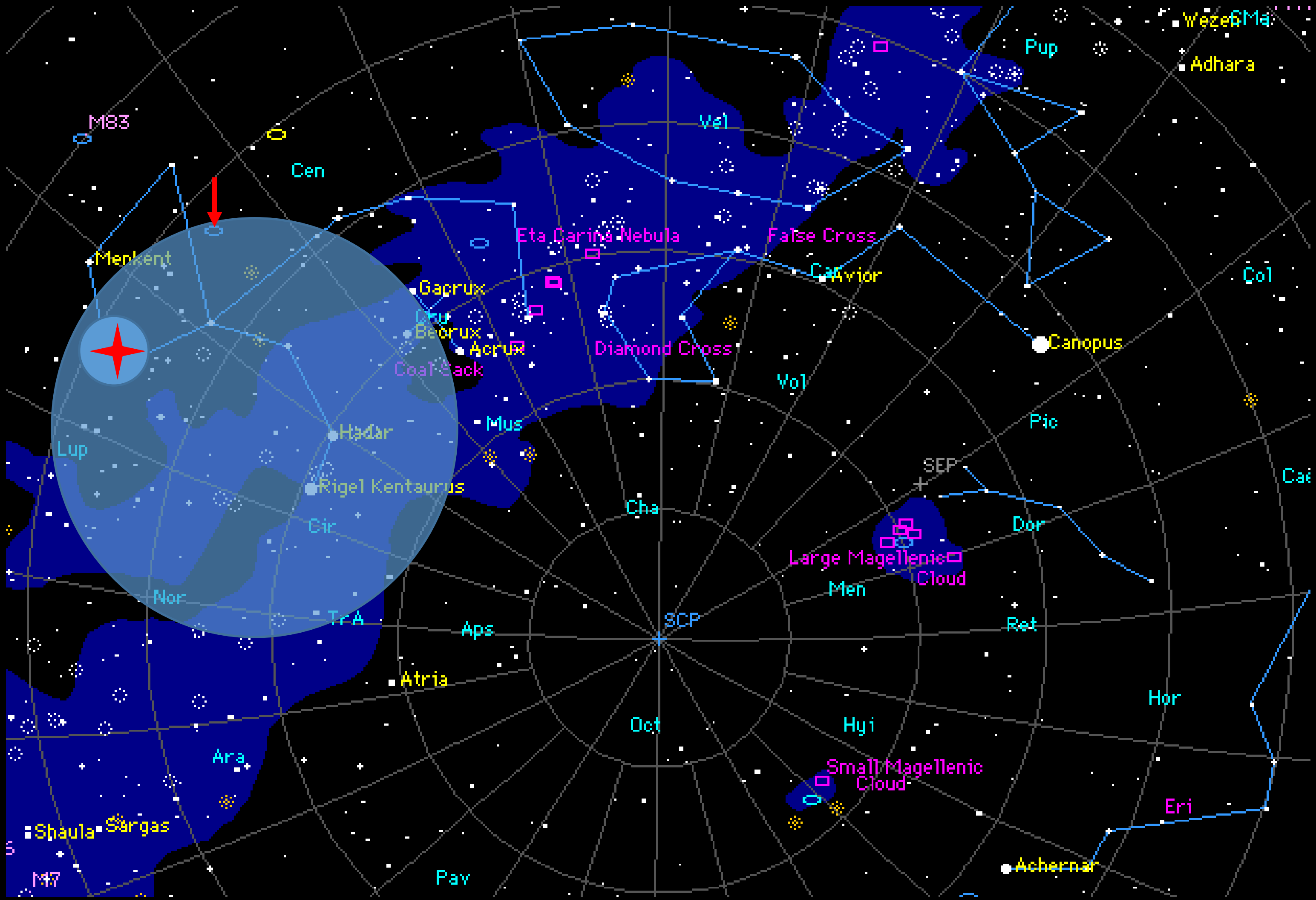
M83
Cen
Menkent
Gacrux
Cru
Becrux
Acrux
Coal Sack
Eta Carina Nebula
Vel
Pup
Adhara
False Cross
Car
Avior
Diamond Cross
Canopus
Col
Vol
Pic
Mus
Hadar
Rigel Kentaurus
Lup
Cir
Nor
TrA
Aps
Cha
SEP
Dor
Large Magellenic
Cloud
Men
SCP
Ret
Cae
Atria
Oct
Hyi
Hor
Small Magellenic
Cloud
Eri
Ara
Shaula
Sargas
Pav
Achernar
M7

Epoch of Reionization

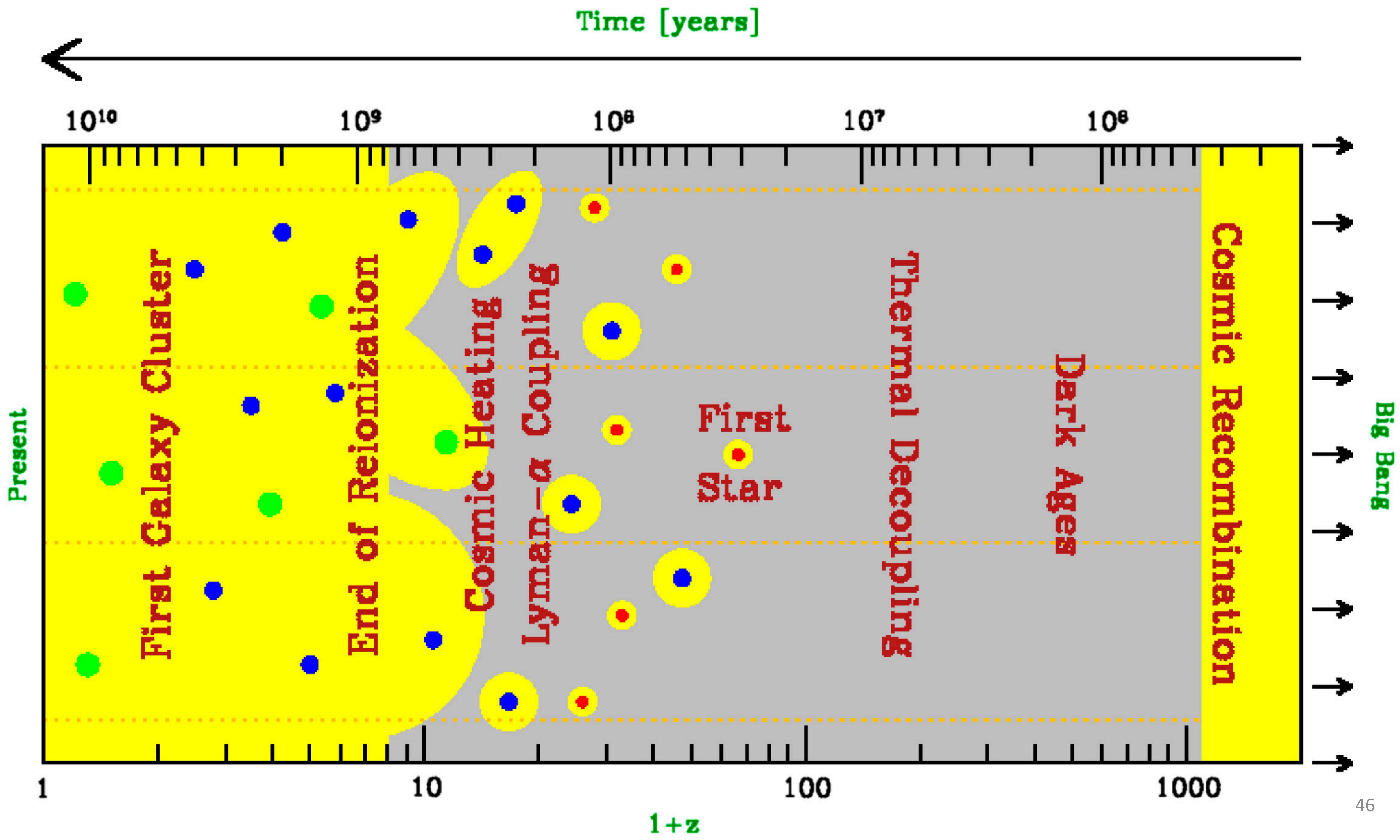
Time [years]
10^10
10^9
10^8
10^7
10^6
Present
First Galaxy Cluster
End of Reionization
Cosmic Heating
Lyman-α Coupling
First Star
Thermal Decoupling
Dark Ages
Cosmic Recombination
Big Bang
1
10
100
1000
1+z

HI 21cm Tomography of IGM

Zaldarriaga + 2003

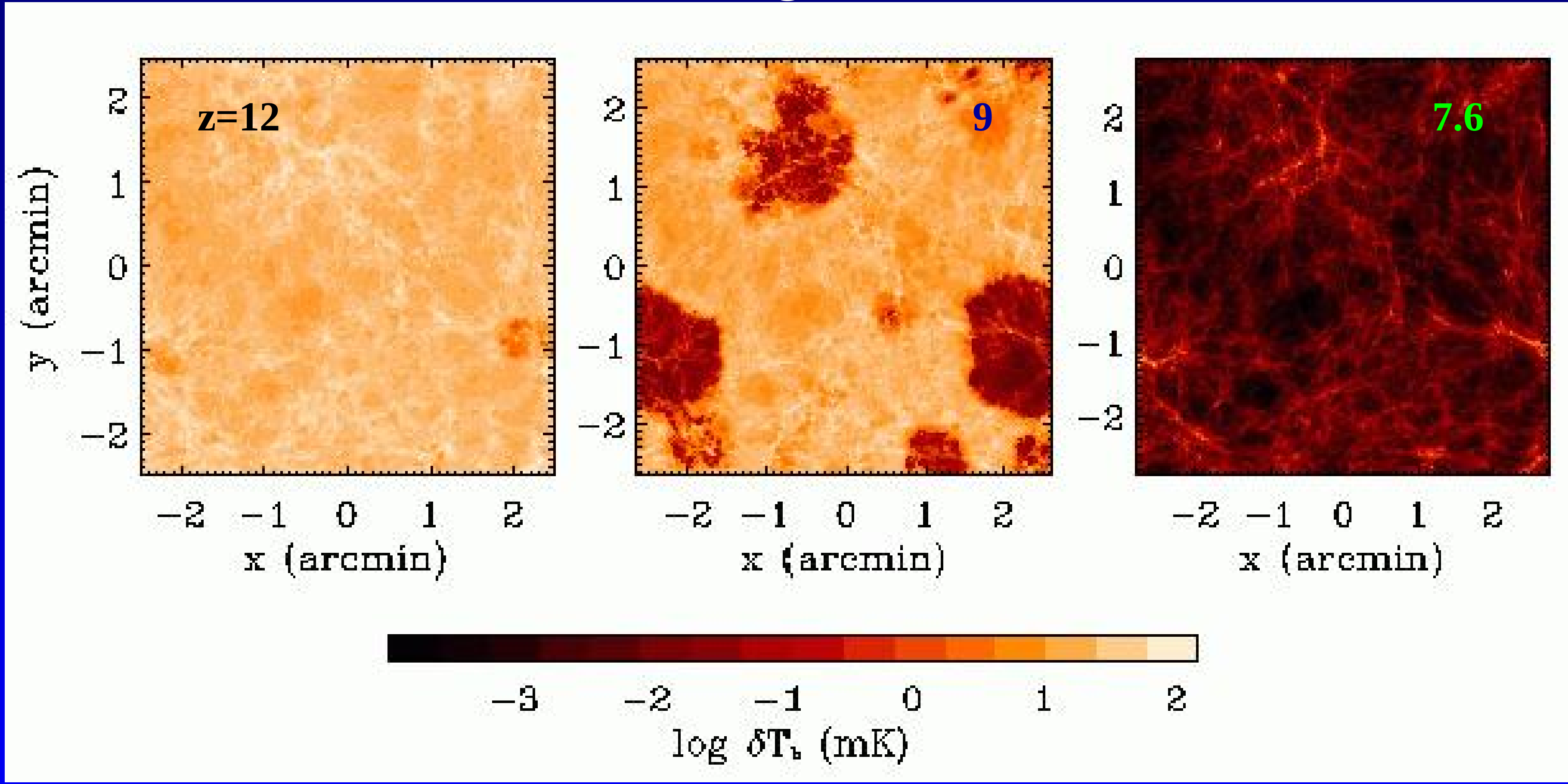

- ΔT_B (2 arcmin) = 10-30 mK
- SKA rms (100hr) = 4mK
- LOFAR rms (1000hr) = 80mK

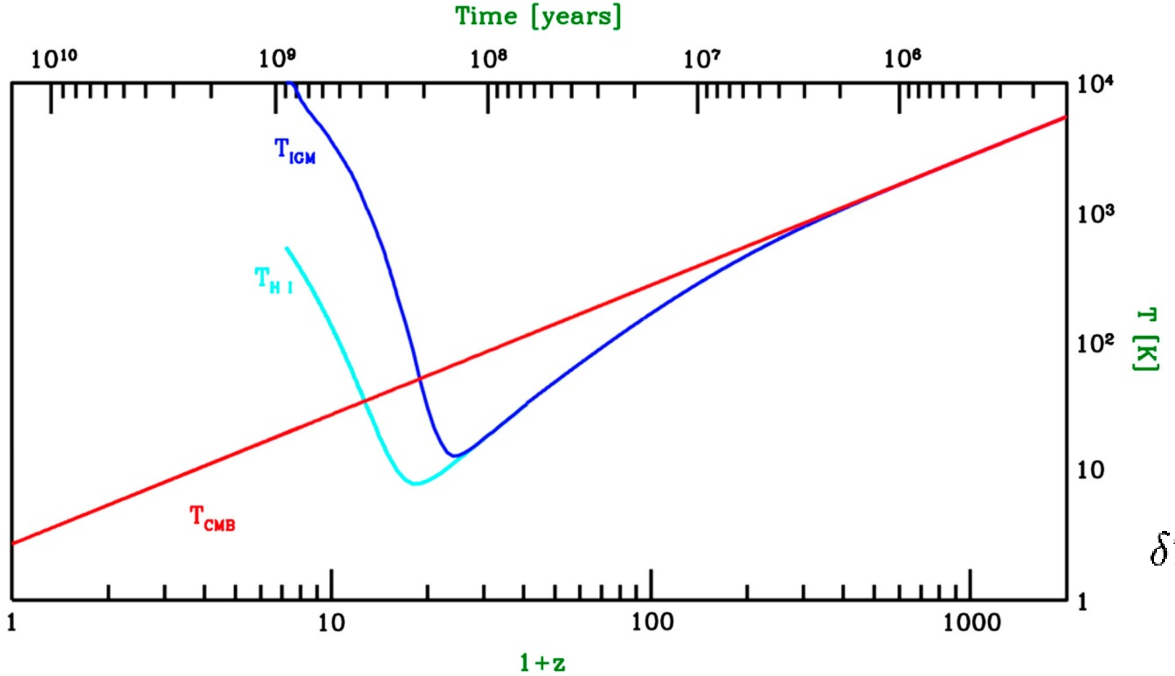

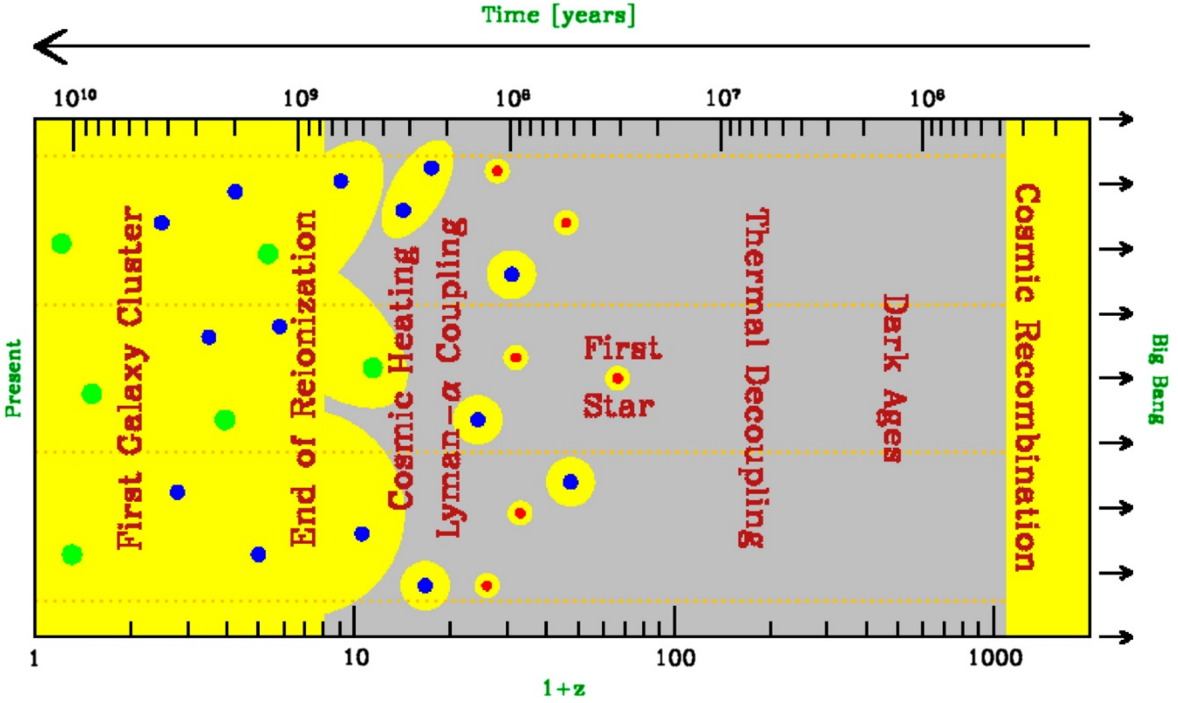

$$\delta T_b(\nu) = \frac{T_S - T_\gamma(z)}{1+z}(1 - e^{-\tau_{\nu 0}}) \approx \frac{T_S - T_\gamma(z)}{1+z}\,\tau_{\nu 0}$$
$$\approx 9\; x_{\rm HI}(1+\delta)\,(1+z)^{1/2}\left[1 - \frac{T_\gamma(z)}{T_S}\right]\left[\frac{H(z)/(1+z)}{{\rm d}v_{||}/{\rm d}r_{||}}\right]\;{\rm mK}.$$

Theoretical reionization signature

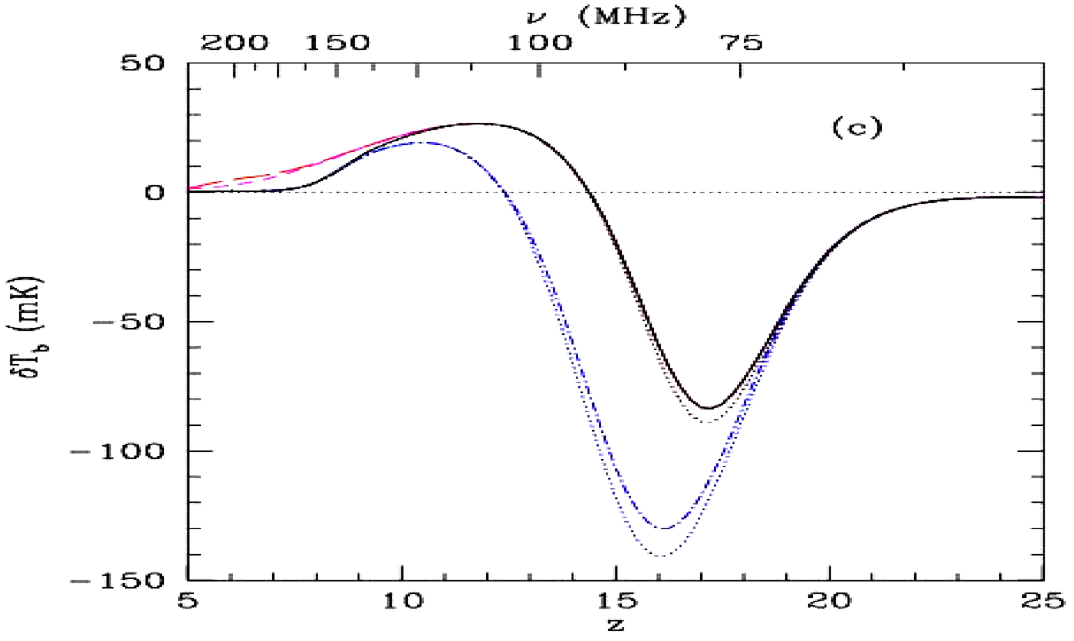

Furlanetto, Oh, Briggs 06

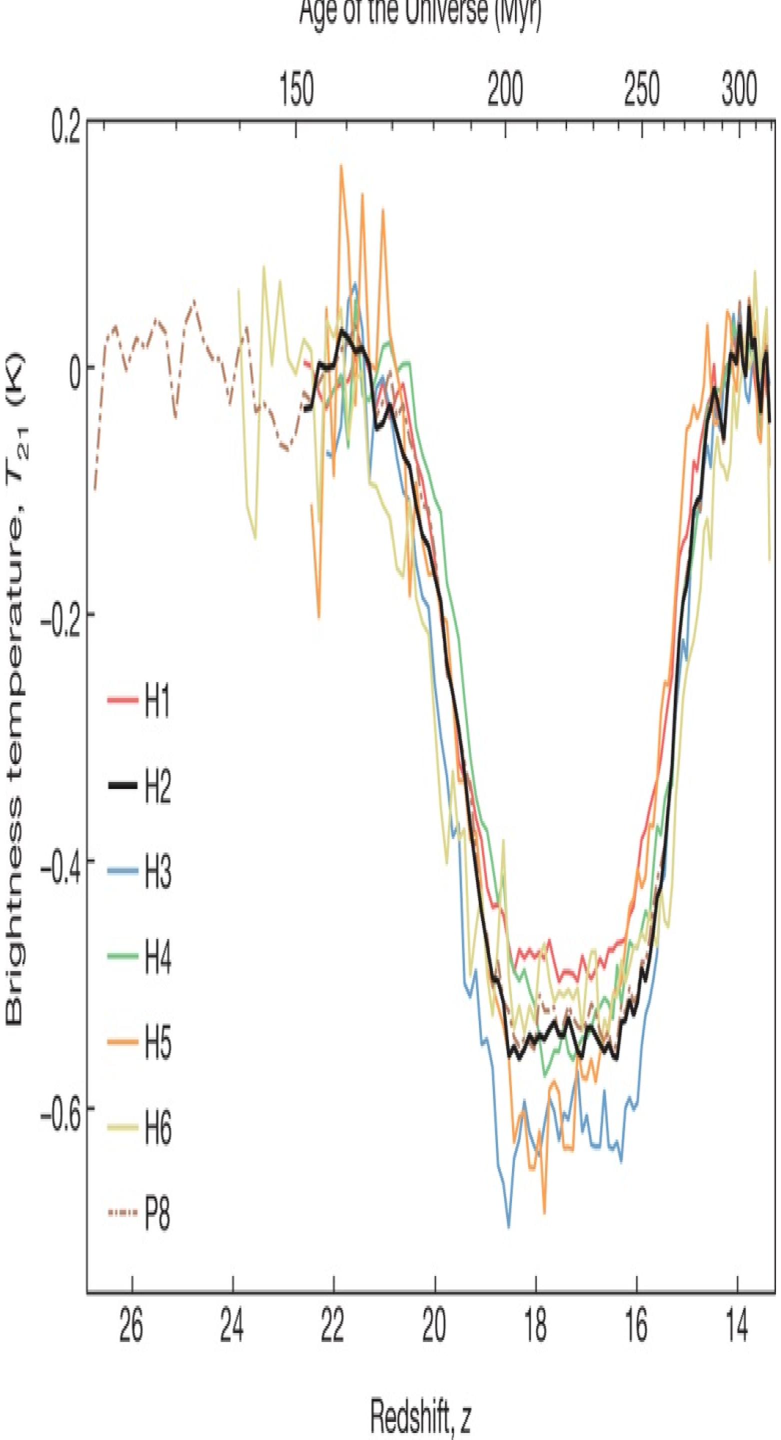

This represents an unexpectedly deep absorption, compared to the expectation within the standard model (Pritchard & Loeb 2012). To explain the strength of the absorption signal, the primordial gas must have been colder than expected. Any astrophysical phenomena could only have acted to raise the IGM gas temperature, such as the heating from early sources of X-ray radiation (e.g. Jeon et al. 2012), and thus cannot explain it.

Bowman, Rogers, et al., 2018

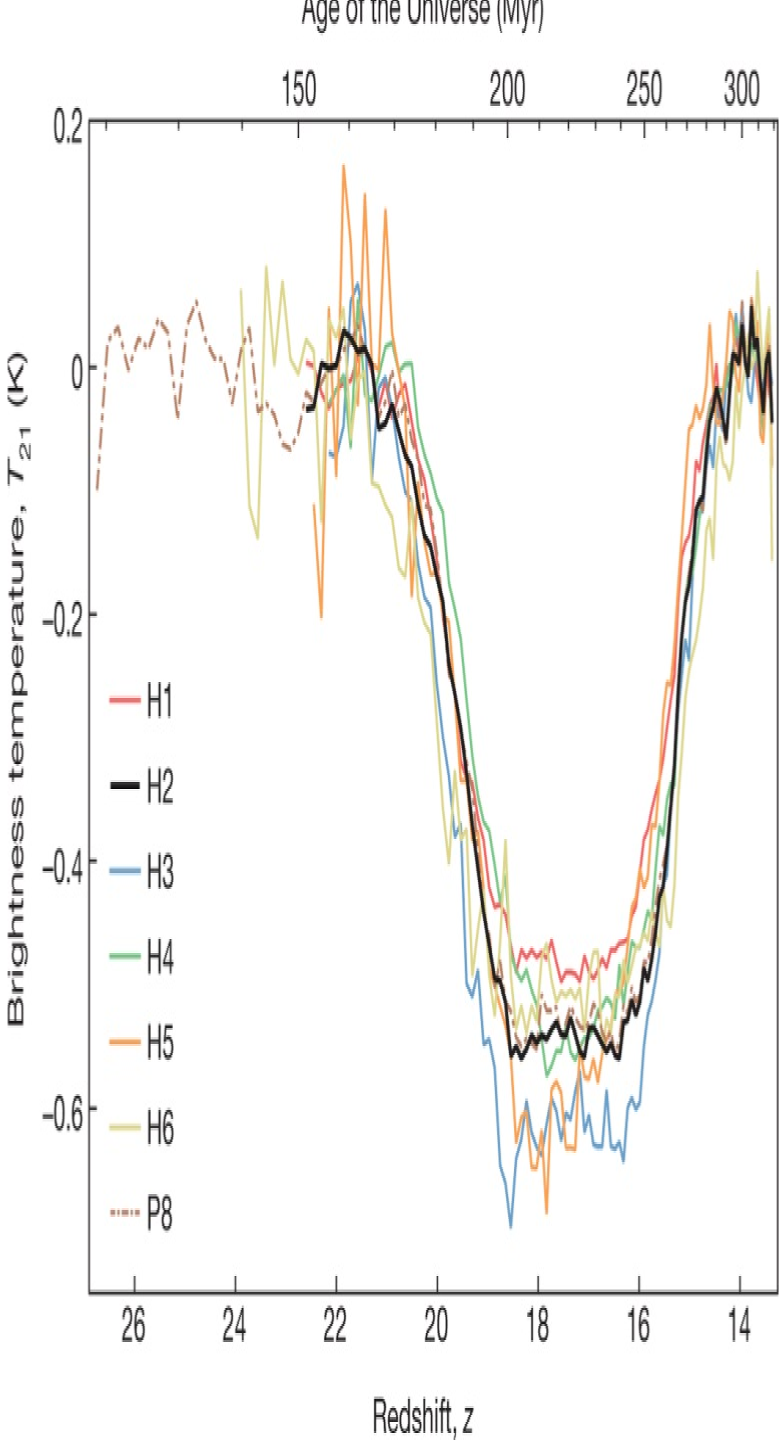

Remarkably, the peak amplitude of the absorption is 3 – 5 times larger than predicted by the most optimistic models, and the absorption profile is flat-bottomed, rather than curvilinear and Gaussian-like, which is also at odds with models.

So how can the differences from the models be explained?

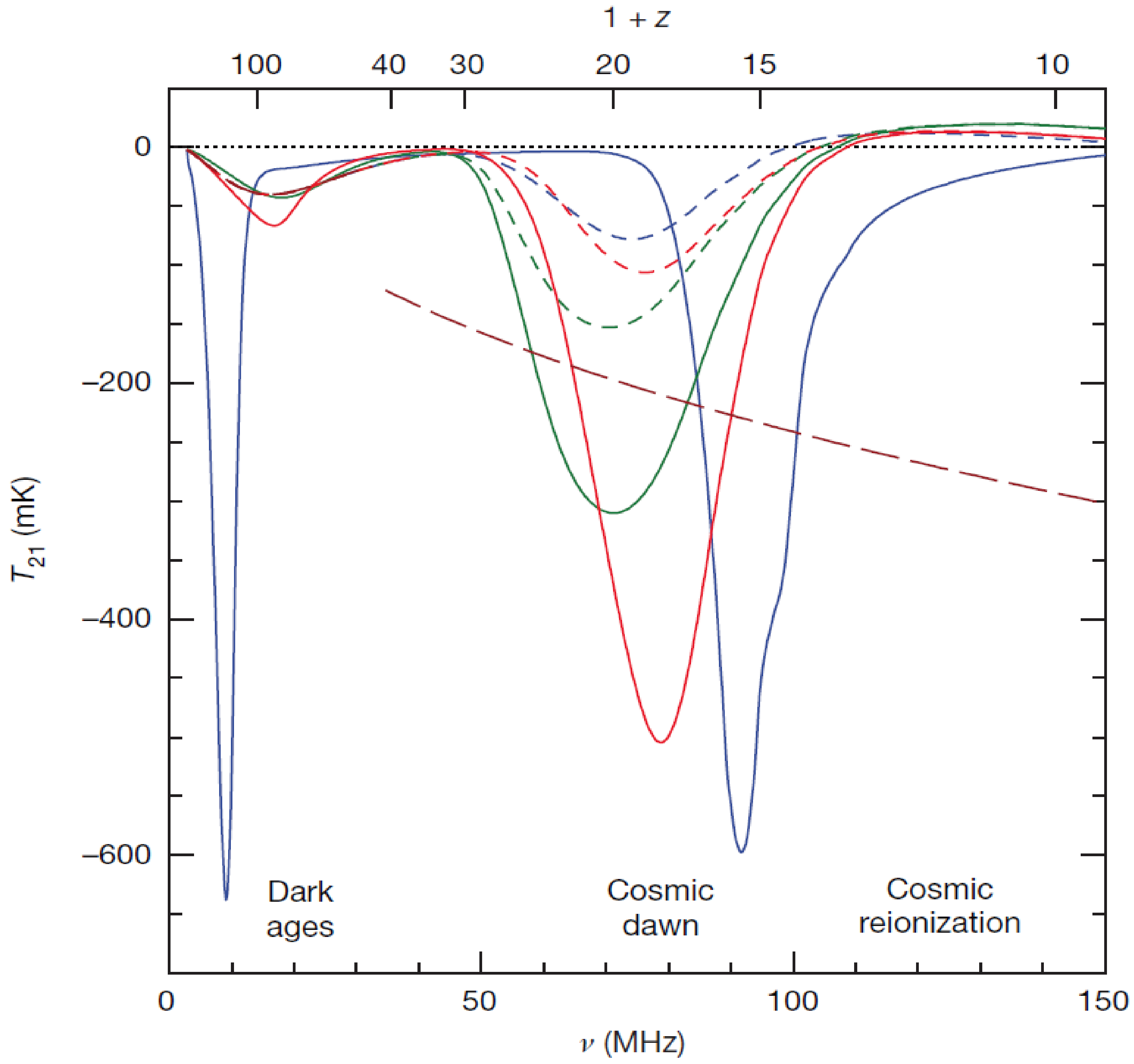

Figure 2 | Global 21-cm signal in models with baryon–dark matter scattering. The globally averaged 21-cm brightness temperature T_{21} (in millikelvin) is shown at an observed frequency ν (in megahertz), with the corresponding value of $1+z$ displayed at the top. We chart some of the space of possible 21-cm signals (see Methods for a discussion on their shapes) using three models (solid curves), with: $\sigma_1 = 8 \times 10^{-20}$ cm^2 and $m_\chi = 0.3$ GeV (red; roughly matching the most likely observed value[5] of the peak absorption); $\sigma_1 = 3 \times 10^{-19}$ cm^2 and $m_\chi = 2$ GeV (green); and $\sigma_1 = 1 \times 10^{-18}$ cm^2 and $m_\chi = 0.01$ GeV (blue). The astrophysical parameters assumed by these models are given in Methods. The corresponding 21-cm signals in the absence of baryon–dark matter scattering are shown as short-dashed curves. Also shown for comparison (brown long-dashed line) is the standard prediction for future dark ages measurements assuming no baryon–dark matter scattering for $\nu < 33$ MHz (matches all the short-dashed curves in this range) and the lowest global 21-cm signal at each redshift that is possible with no baryon–dark matter scattering, regardless of the astrophysical parameters used (for $\nu > 33$ MHz).

Rennan Barkana (2018)

Bowman and Rogers conducted myriad tests in which the they altered their experimental hardware or data analysis.

The tests included

- repeating the data acquisition and analysis using a duplicate antenna at a second, nearby location;
- orienting the antenna at different azimuth;
- changing the ways in which the antenna is isolated from the ground
- switching various facets of the data calibration on and off.

ASU Arizona State University

ASU Home ▾ My ASU Colleges and Schools ▾ Map and Locat

School of Earth and Space Exploration

🏠 Degree Programs ▾ Why Study Here? Research ▾ Public Engagement ▾ People ▾ Student Life ▾ Admission ▾ About ▾

Judd Bowman

Judd.Bowman@asu.edu 480-965-8880

ISTB4-675 Tempe

School Of Earth and Space Exploration

Associate Professor

Faculty, TEMPE Campus, Mailcode 6004

Bio | Research | Teaching

Alan Rogers

Haystack's Alan Rogers wins Reber Medal

July 14, 2010

RELATED

MIT Haystack Observatory

The 2010 Grote Reber Gold Medal for outstanding and innovative contributions to radio astronomy was presented this month to Alan Rogers, a research affiliate at MIT's Haystack Observatory. The award recognizes Rogers' many pioneering developments in radio and radar interferometry, radio spectroscopy, and for his application of radio astronomy techniques to society.

327 MHz line of interstellar deuterium

The EDGES Experiment

The Experiment to Detect the
Global EOR Signature (EDGES)

2012

2017

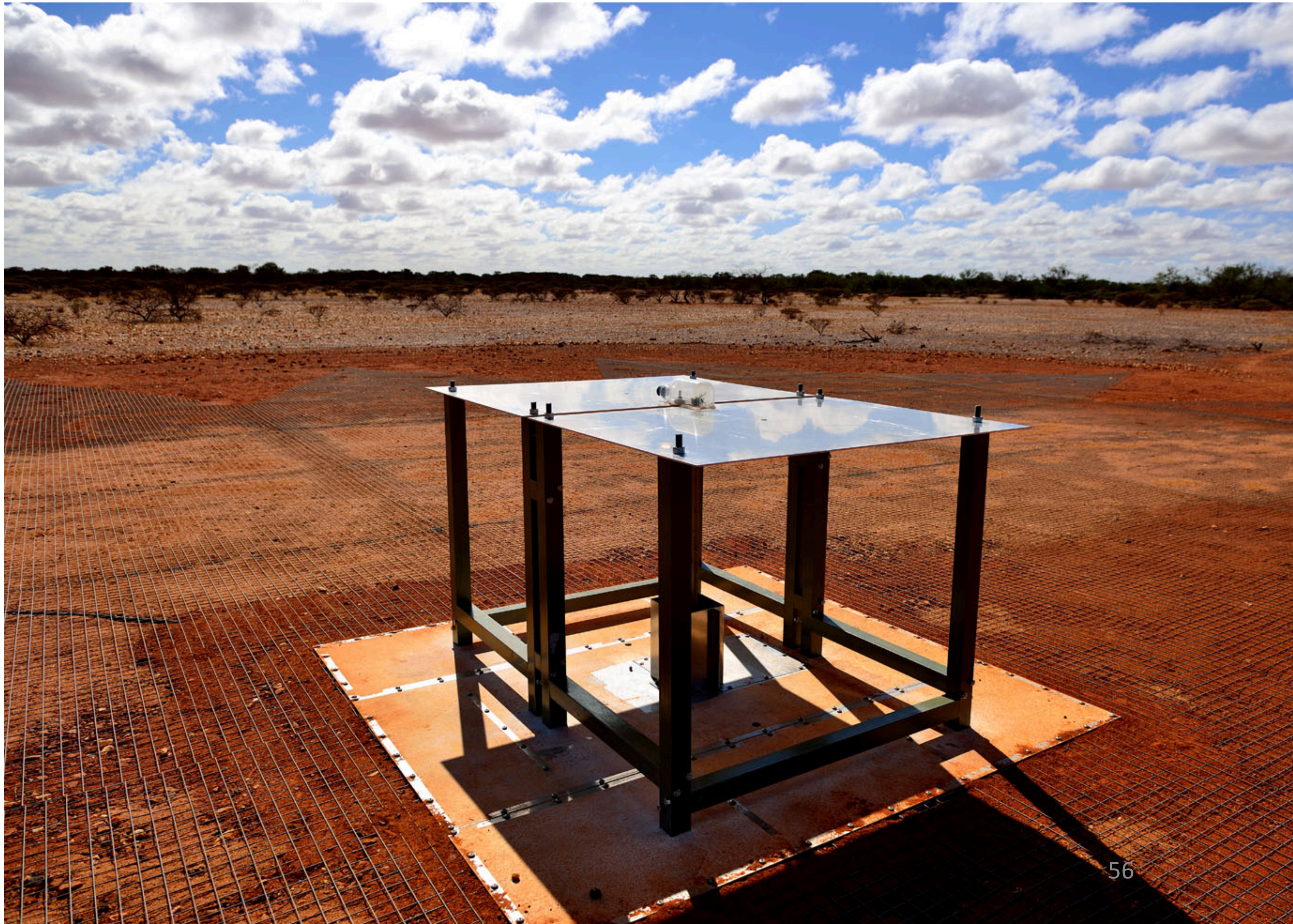

**LOFAR (Low-frequency Array)*

Netherlands/Europe

**MWA (Murchison Wide-Field Array)*

MIT/U.Melbourne,ATNF,ANU/CfA/Raman I.

**PAPER*

UCB, South Africa

**21CMA (formerly known as PAST)*

China

**GMRT (Giant Meterwave Radio Telescope)*

India/CITA

**SKA (Square Kilometer Array)*

International

So how to explain unexpected depth and shape of the signal?

Barkana (2018) argues that models could achieve the reported signal amplitude and profile if non-gravitational interactions occur between dark matter and normal matter particles, and if the dark-matter particles have relatively low masses and velocities that are less than the speed of light.

The idea that a detectable radio signal from the cosmic dawn can be connected to the particle properties of dark matter suggests a potentially revolutionary angle for exploring fundamental physics.

Greenhill (Nature, 2018)

The most stringent test will be to compare the current results with those to come from independent experiments also aimed at detecting the cosmic-dawn signal. I hope that the unexpected amplitude and line shape of the reported absorption signal is indeed a hard-won breakthrough that reveals evidence of unexpected physics.

Greenhill, 2018

Role of SKA: Refining the measurements; measuring properties of the dark matter; looking at a higher frequency emission feature; detecting fluctuations due to RRLs and primordial fluctuations; applying a 3D tomography approach, etc, etc.

3D Tomography of Neutral Hydrogen

- Movie 1 (As we change frequency – the SKA as a time machine)
- Movie 2 (God's eye view)

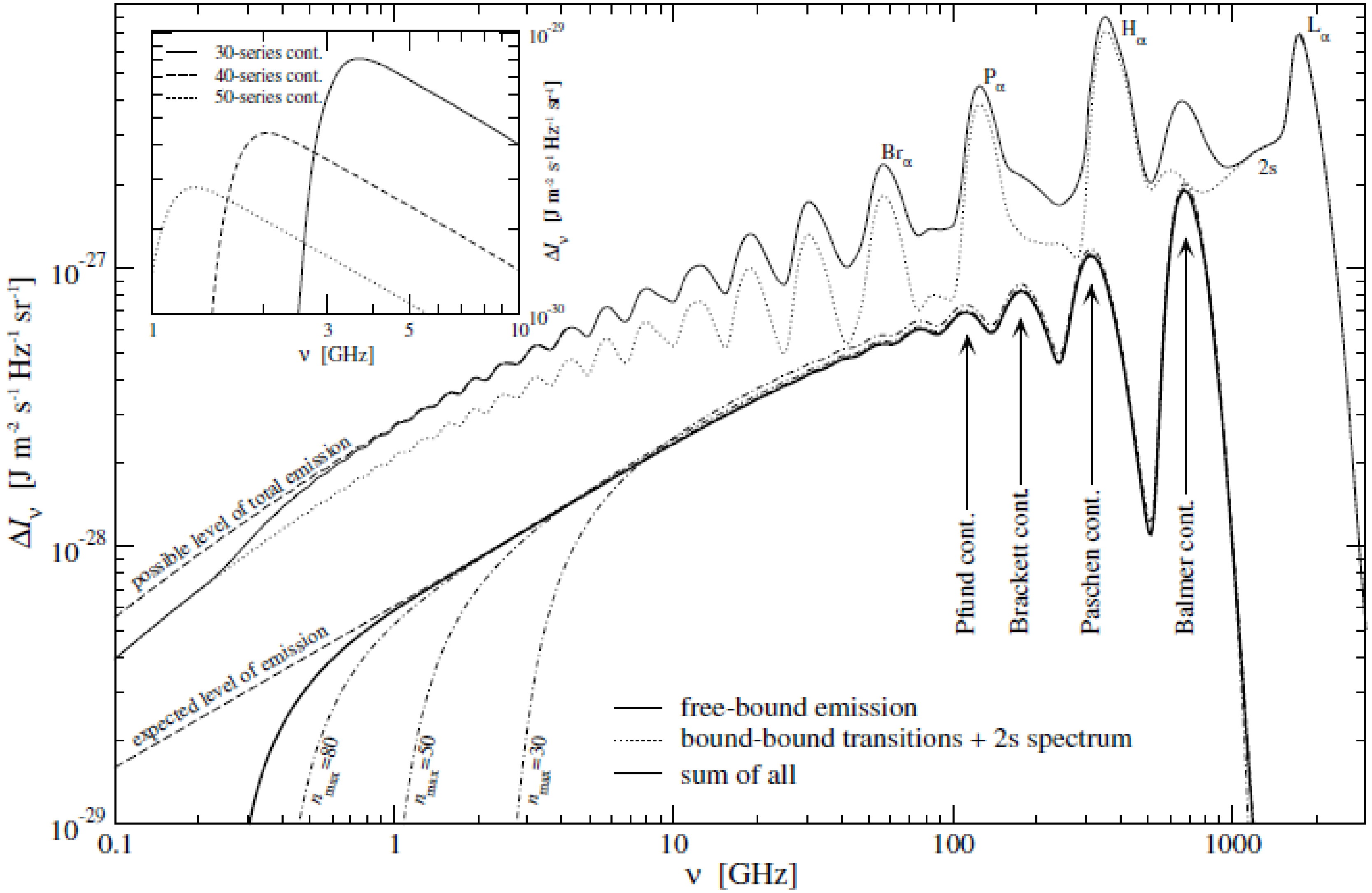

R. A. Sunyaev, and J. Chluba 2009

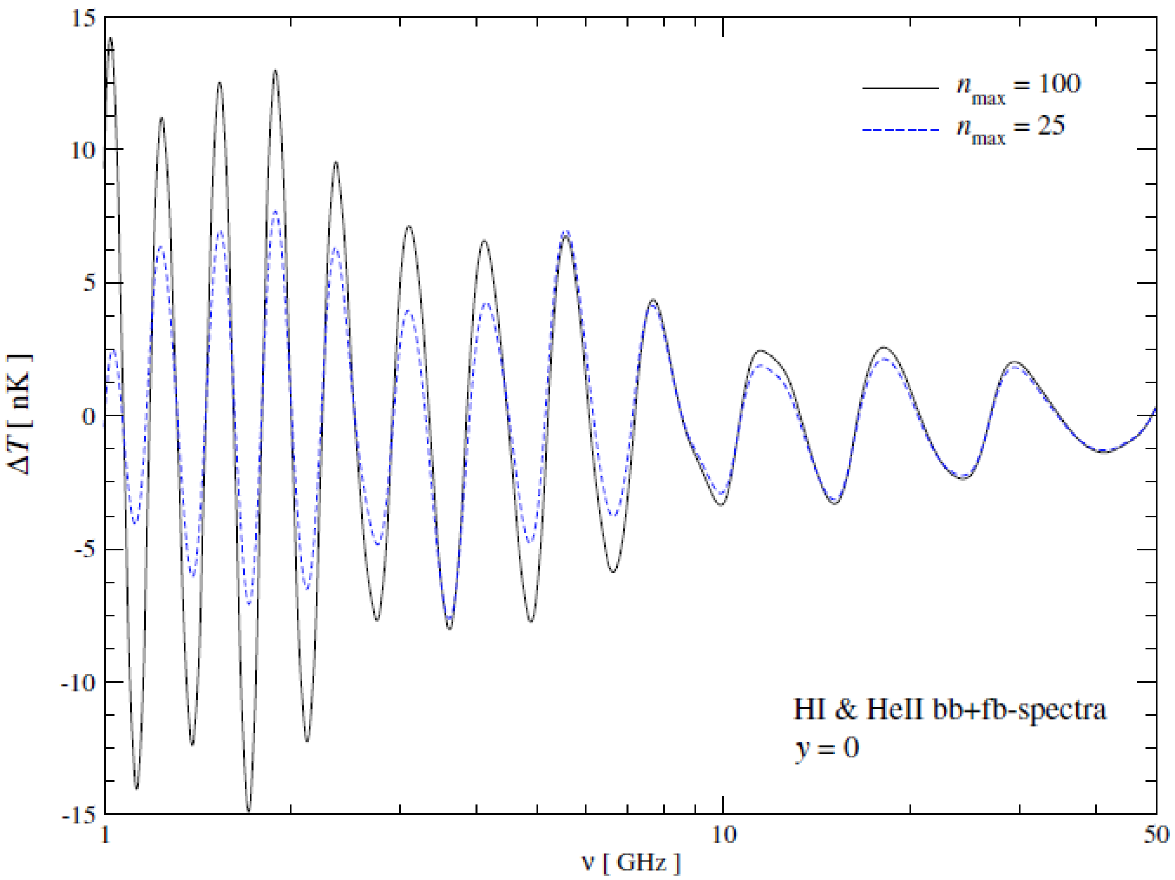

Fig. 9 (online colour at: www.an-journal.org) Frequency-dependent modulation of the CMB temperature caused by photons from the H I and He II recombination epochs. Both the bound-bound and free-bound contributions were included, and the mean recombination spectrum was subtracted. The shown signal is practically *unpolarized* and the same in *all* directions on the sky. The figure is taken from Chluba & Sunyaev (2008c).

Stars in the telescopic eye: LVHIS and the nearby Universe

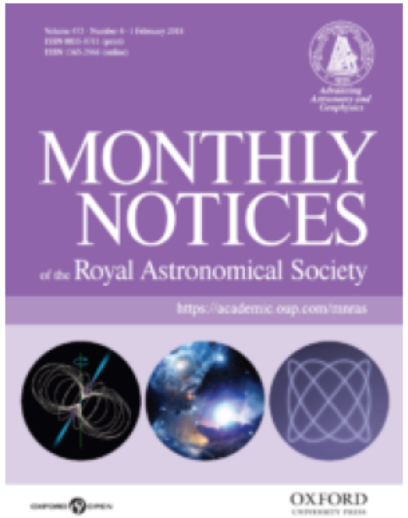

BY BÄRBEL KORIBALSKI (HTTPS://BLOG.OUP.COM/AUTHORS/BARBEL-KORIBALSKI/)

JULY 9TH 2018

Spiral galaxies like the Milky Way and its neighbour, the Andromeda Galaxy, contain about 100 billion stars each, the light of which can be seen by eye. Also visible are small amounts of dust, typically enshrouding the sites of young star formations. What cannot be seen by the naked eye are the vast amounts of cold hydrogen gas and even larger reservoirs of dark matter. These elements of galaxy make-up are detectable only by radio telescopes.

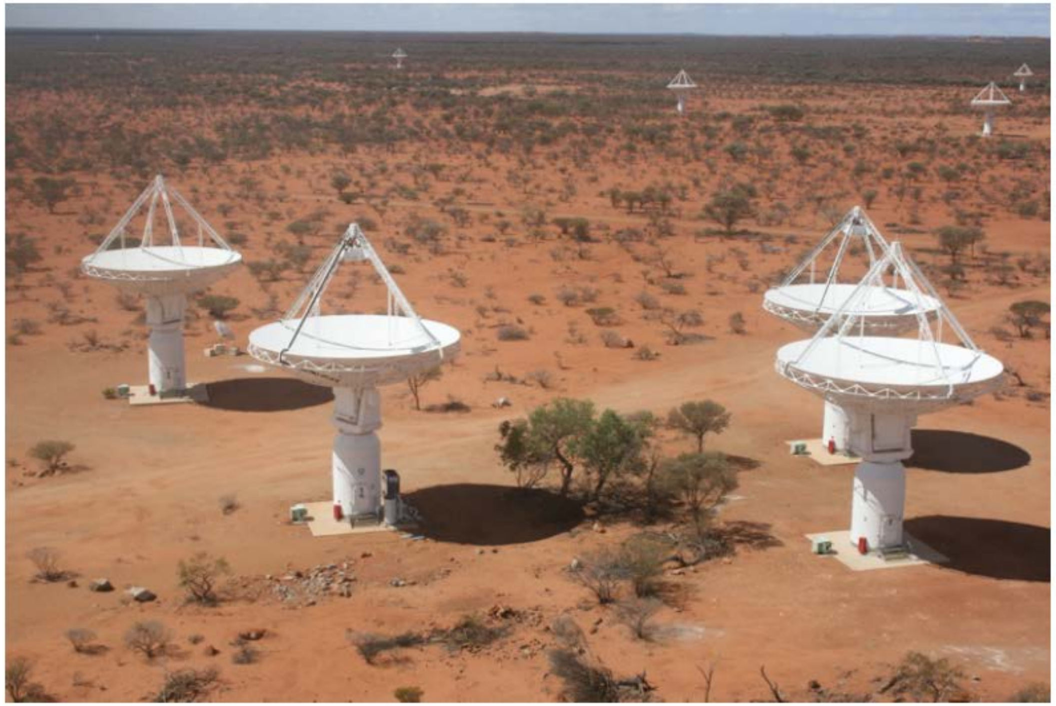

Image credit: The Australian Square Kilometre Array Pathfinder (ASKAP) by Simon Johnston. Used with permission.

The project is called LVHIS—pronounced ELVIS—which stands for Local Volume HI Survey (http://www.atnf.csiro.au/research/LVHIS/). While the Milky Way and Andromeda Galaxy—together with about 100 small neighbours known as dwarf galaxies —make up the Local Group, the Local Volume (LV) encompasses around 1000 nearby galaxies out to a distance of 30 million light years. We chose to analyse galaxies already detected with CSIRO's Parkes 64-m telescope (http://www.parkes.atnf.csiro.au/) (known as "The Dish") in the HI Parkes All Sky Survey (HIPASS) (http://www.atnf.csiro.au/research/multibeam/). Using these pre-detected galaxies allowed us to map their hydrogen structure with 20 times greater accuracy, and to derive their rotation speeds, which are important for measuring dark matter content.

ASKAP Projects: WALLABY, GASKAP, EMU

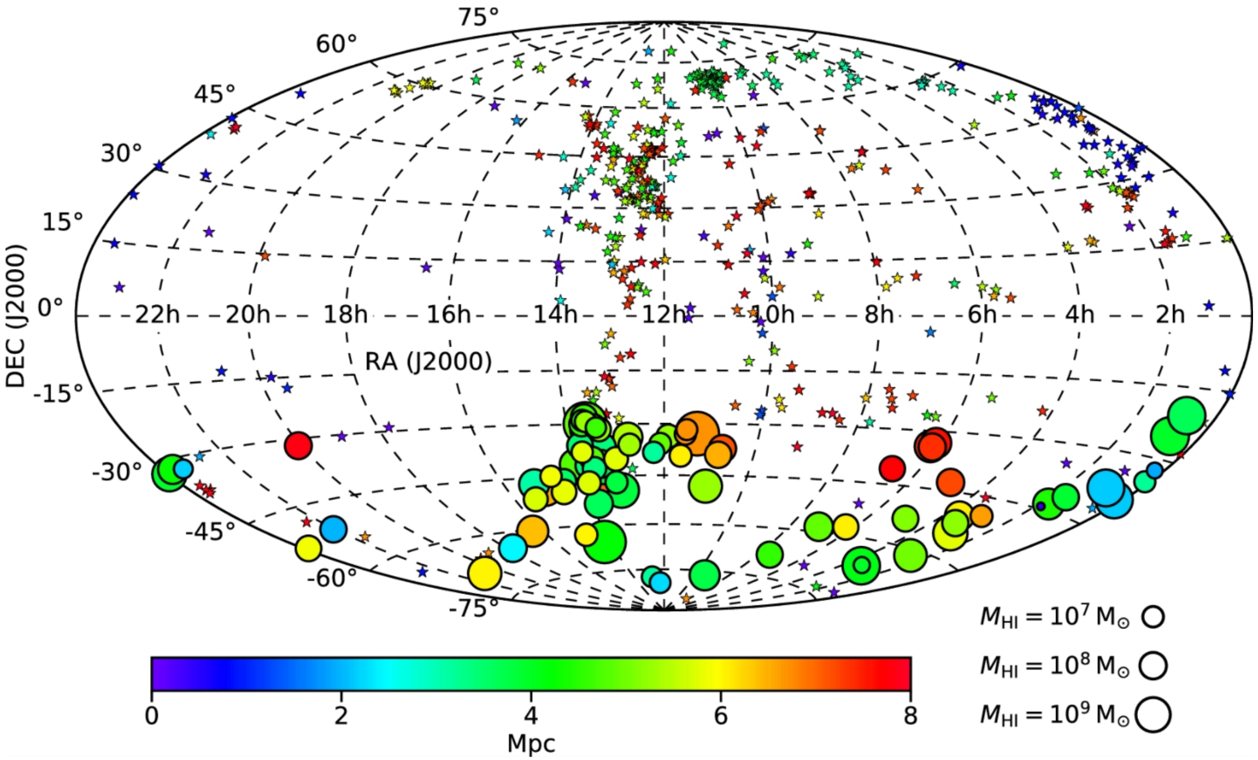

From: The Local Volume H i Survey (LVHIS)

Mon Not R Astron Soc. 2018;478(2):1611-1648. doi:10.1093/mnras/sty479

Hydrogen in Galaxies

The Local Volume HI Survey (LVHIS) * Koribalski et al. 2018

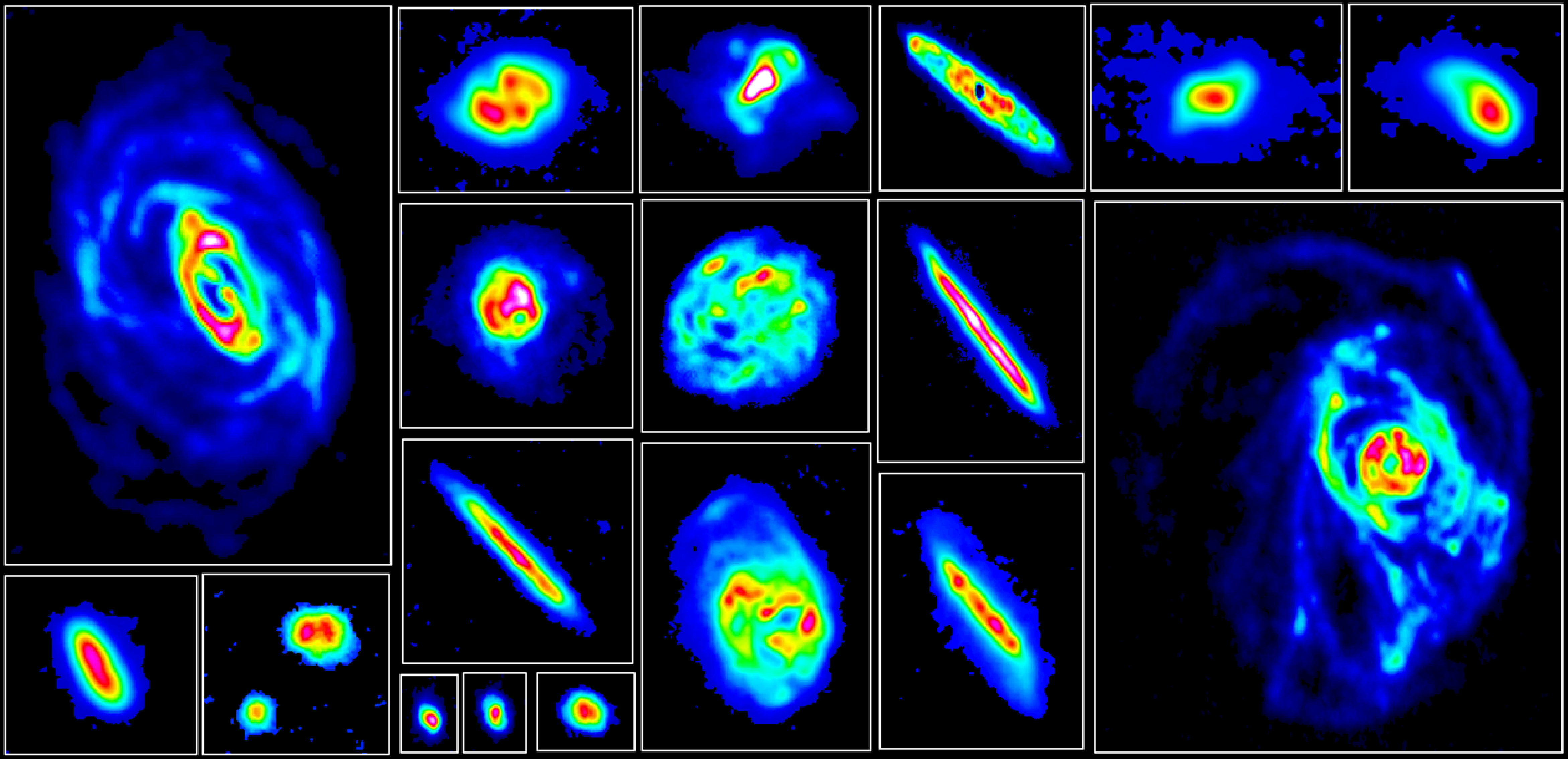

CSIRO's Australia Telescope Compact Array

Hydrogen in Galaxies

The Local Volume HI Survey (LVHIS) * Koribalski et al. 2018

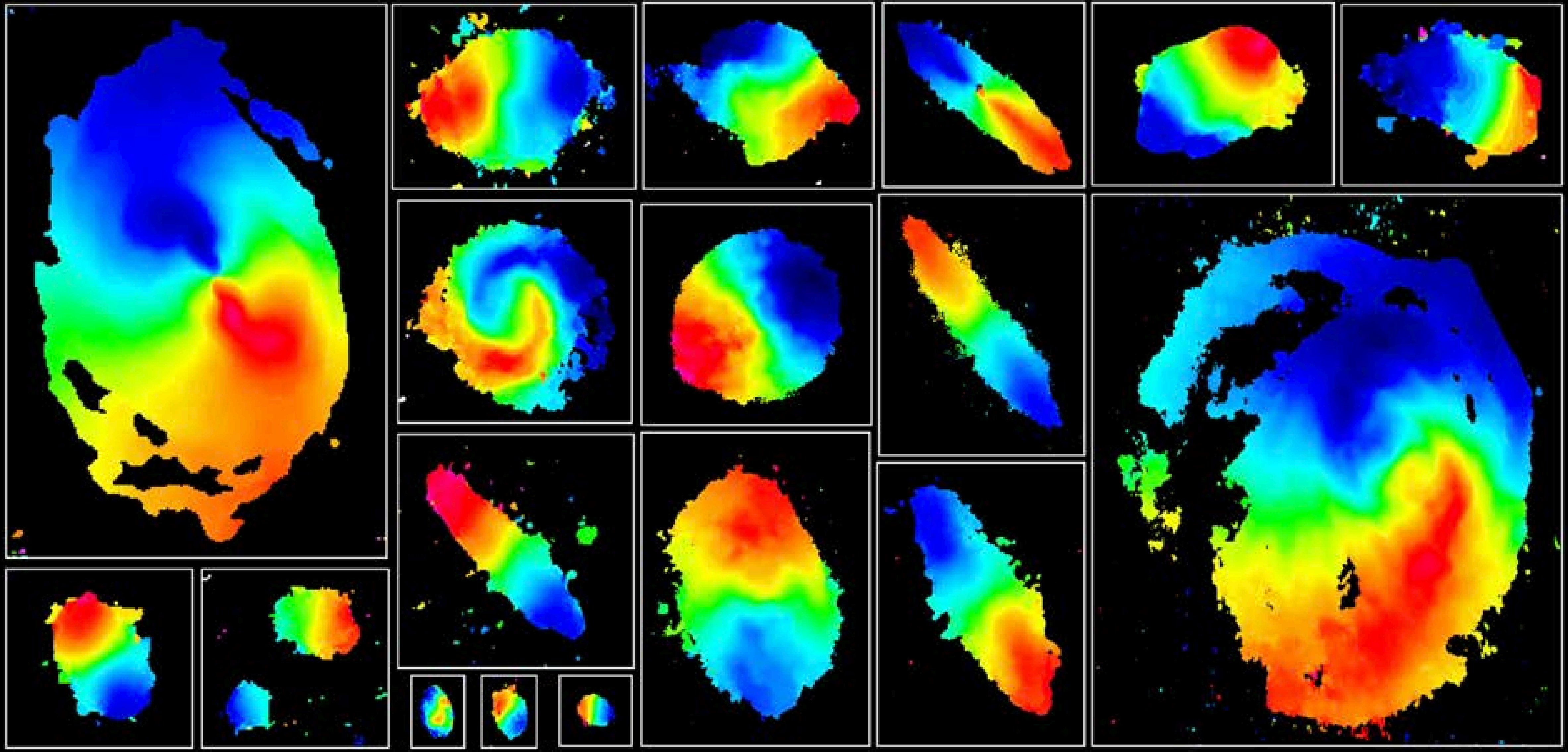

CSIRO's Australia Telescope Compact Array

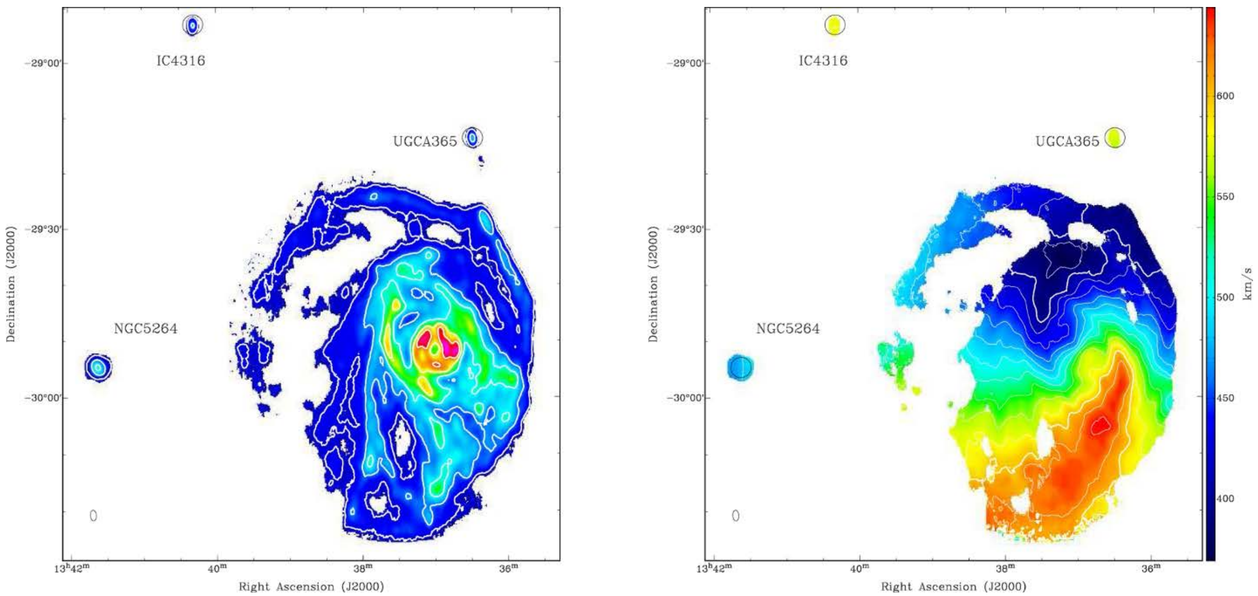

From: The Local Volume H i Survey (LVHIS)

Mon Not R Astron Soc. 2018;478(2):1611-1648. doi:10.1093/mnras/sty479

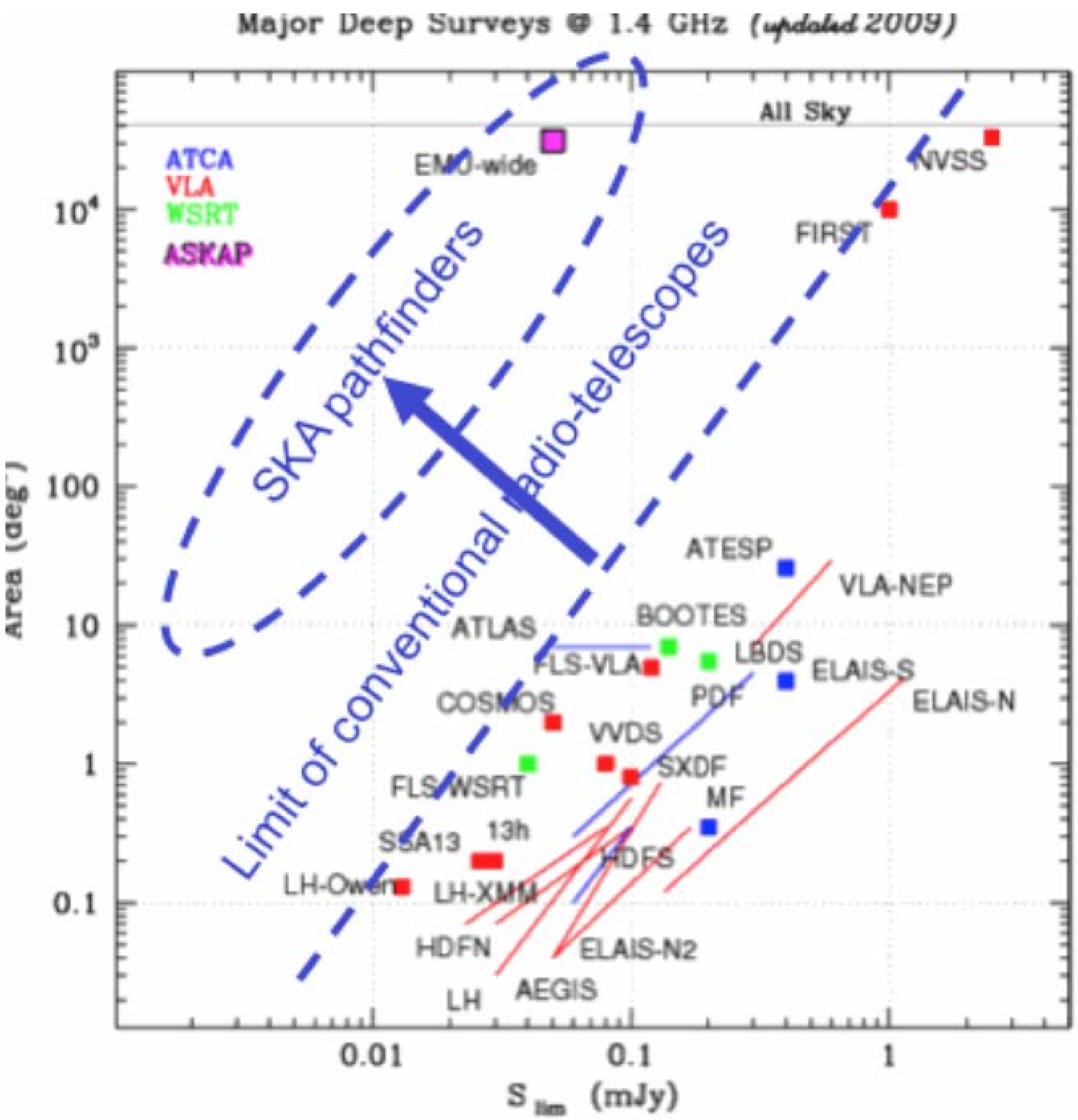
Major Deep Surveys @ 1.4 GHz (updated 2009)
All Sky
ATCA
VLA
WSRT
ASKAP
EMU-wide
NVSS
FIRST
SKA pathfinders
Limit of conventional radio-telescopes
ATESP
VLA-NEP
BOOTES
ATLAS
LBDS
FLS-VLA
ELAIS-S
PDF
ELAIS-N
COSMOS
VVDS
SXDF
FLS-WSRT
MF
13h
SSA13
HDFS
LH-Owen
LH-XMM
HDFN
ELAIS-N2
AEGIS
LH
Area (deg²)
S lim (mJy)
0.01
0.1
1
0.1
1
10
100
10³
10⁴

- SKA-1 will allow to extend the volume studied in this “pathfinder” survey by the factor of 100-1000, therefore to increase by the same factor number of galaxies studied, providing important data for the study of the dark matter content in galaxies at different epochs.

THANK YOU!

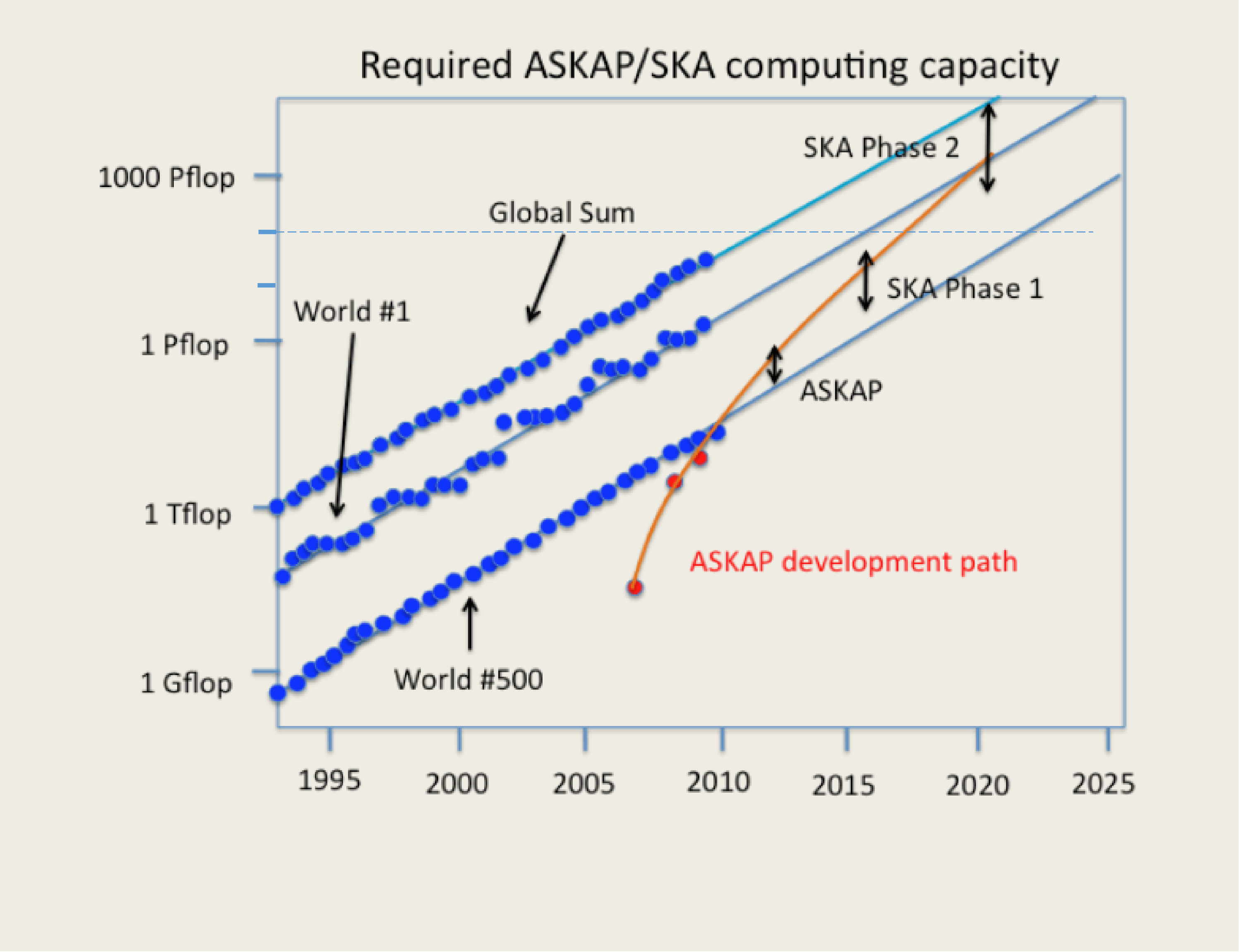

Figure 3: Available computing power over time compared with ASKAP and SKA data needs, adapted from a figure by Tim Cornwell. The three lines show the world's fastest computer, the world's 500th most powerful computer, and the sum of the top 500 computers.

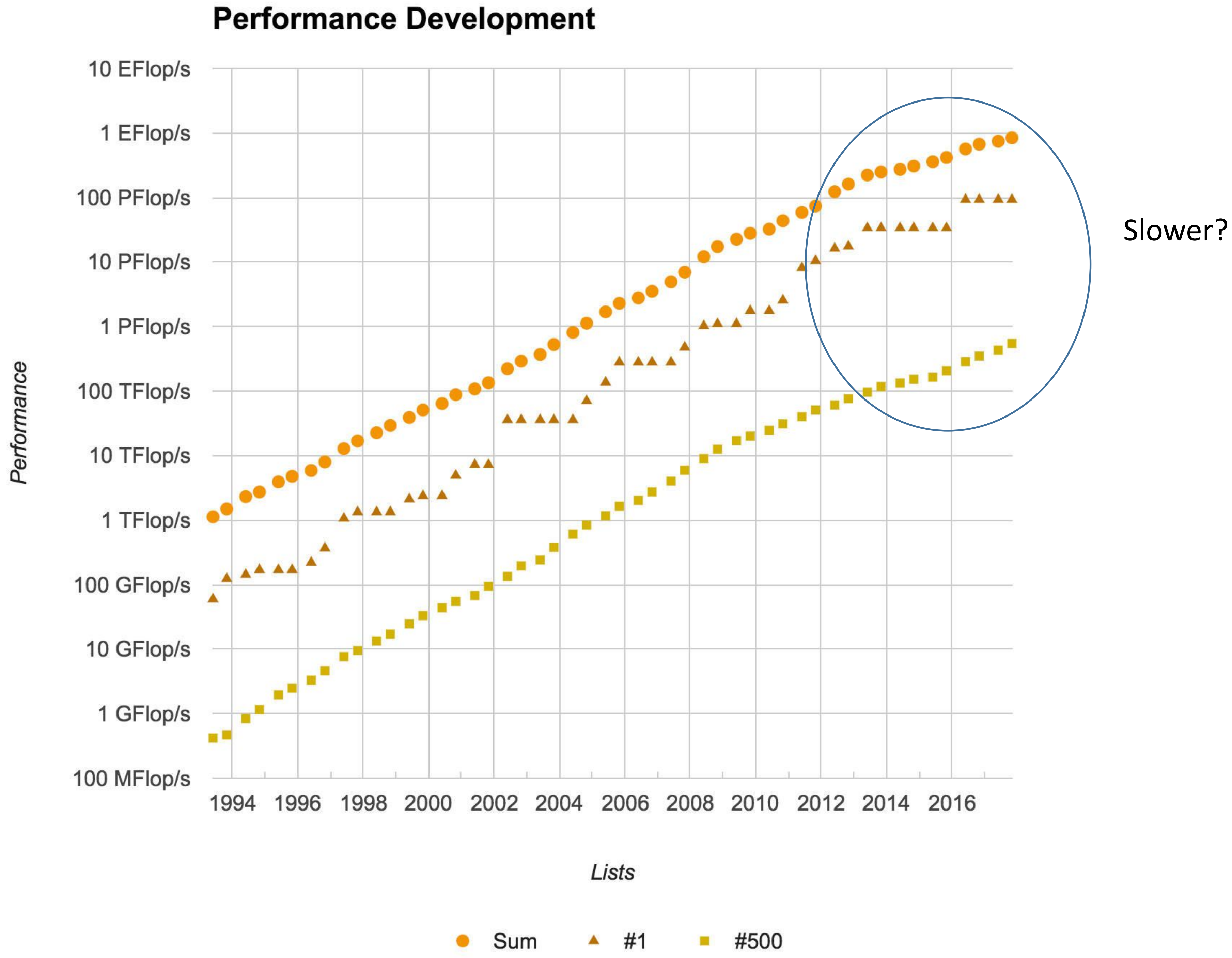
Performance Development
10 EFlop/s
1 EFlop/s
100 PFlop/s
10 PFlop/s
1 PFlop/s
100 TFlop/s
10 TFlop/s
1 TFlop/s
100 GFlop/s
10 GFlop/s
1 GFlop/s
100 MFlop/s
Performance
1994
1996
1998
2000
2002
2004
2006
2008
2010
2012
2014
2016
Lists
Sum
#1
#500
Slower?

TABLE I. POWER PROJECTIONS FOR DIFFERENT SKA SUBSYSTEMS AND PHASES; TARGET : <**100MW.**

SKA Phase 1 and 2	***South Africa***	***Australia***
Sparse Arrays		3.36 MW
Dishes	1MW	
Dishes/PAF		0.12 MW
On-site Computing	4.7MW	1.32MW
Totals/site	5.7MW	4.8MW
SKA Phase2 incl.Dense Arrays	~80MW (SKA Phase 2 configuration not known yet)	
Off-site Computing	~30-40MW (SKA Phase 2 configuration not known yet)	

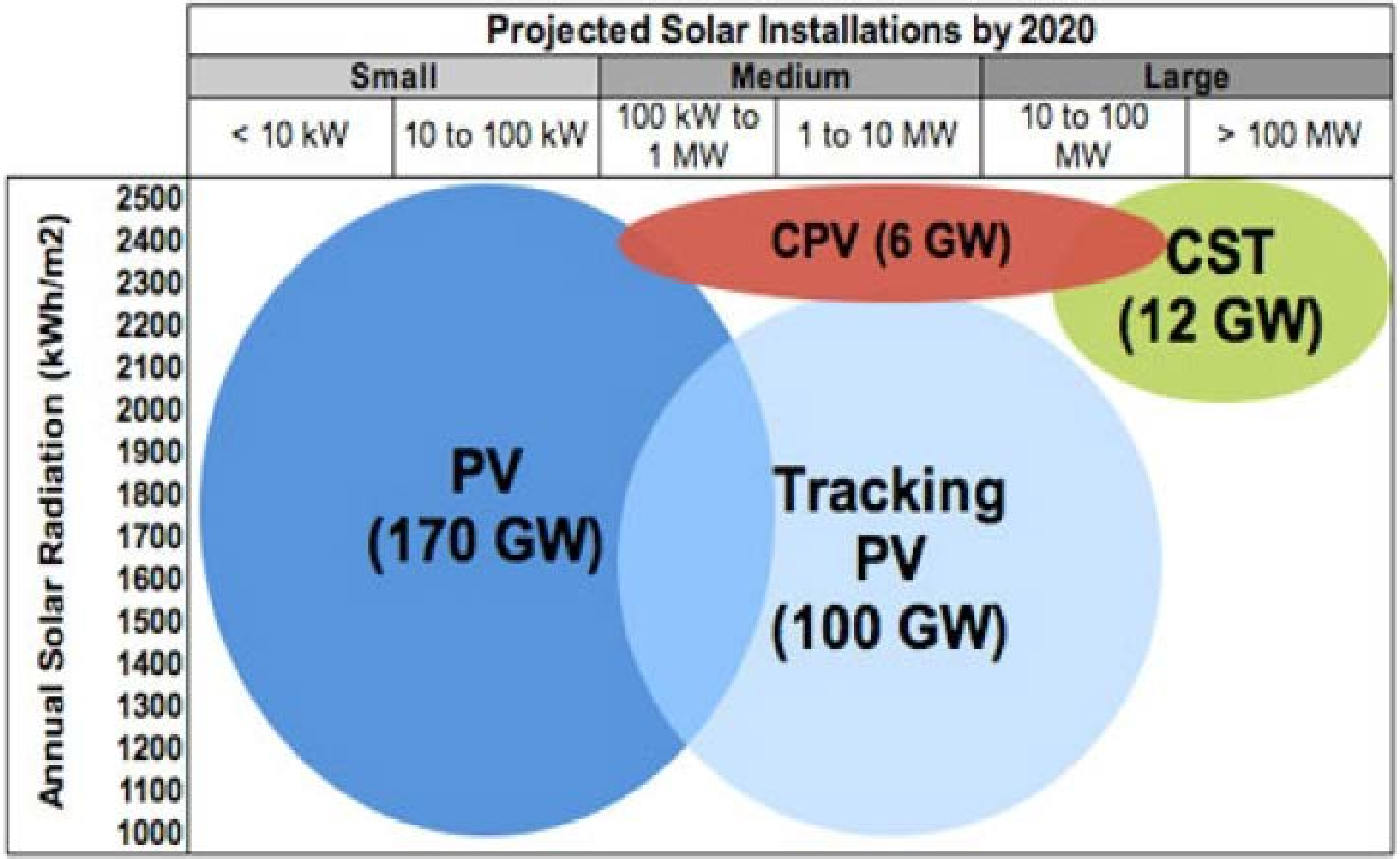

Figure 2. Projections of Solar power market shares by 2020, considering the main technology choices. PV- Photovoltaic; CPV- Concentrated Photovoltaic; CST – Concentrated Solar thermal. From [12].